

# Relativistic and wide-angle corrections to galaxy power spectra

Sheean Jolicoeur<sup>1,a</sup>, Sêcloka L. Guedezounme<sup>2,b</sup>,  
Roy Maartens<sup>2,3,4</sup>, Pritha Paul<sup>5</sup>, Chris Clarkson<sup>5,2</sup>,  
Stefano Camera<sup>6,7,8,2</sup>

<sup>1</sup>Department of Physics, Stellenbosch University, Matieland 7602, South Africa

<sup>2</sup>Department of Physics & Astronomy, University of Western Cape, Cape Town 7535, South Africa

<sup>3</sup>Institute of Cosmology & Gravitation, University of Portsmouth, Portsmouth PO1 3FX, UK

<sup>4</sup>National Institute for Theoretical & Computational Sciences, Cape Town 7535, South Africa

<sup>5</sup>School of Physics & Astronomy, Queen Mary University of London, London E1 4NS, UK

<sup>6</sup>Dipartimento di Fisica, Università degli Studi di Torino, Torino, 10125, Italy

<sup>7</sup>Istituto Nazionale di Fisica Nucleare, Sezione di Torino, Torino, 10125, Italy

<sup>8</sup>Istituto Nazionale di Astrofisica, Osservatorio Astrofisico di Torino, Pino Torinese, 10025, Italy

E-mail: [ajolicoeursheean@gmail.com](mailto:ajolicoeursheean@gmail.com), [seclokaguedezounme@gmail.com](mailto:seclokaguedezounme@gmail.com)

**Abstract.** Galaxy surveys contain information on the largest scales via wide-angle and relativistic contributions. By combining two different galaxy populations, we can suppress the strong cosmic variance on ultra-large scales and thus enhance the detectability of the signals. The relativistic Doppler and Sachs-Wolfe effects are of a similar magnitude to the leading wide-angle corrections, so that it is important to treat them together, especially since they can partially cancel. The power spectra depend on the choice of line of sight for each galaxy pair and we present results for a general line of sight. Then we estimate the detection significance of the auto- and cross-power spectra for a variety of cases. We use two futuristic galaxy samples based on a ‘beyond-DESI’ survey and a SKA Phase 2 survey, covering  $15,000 \text{ deg}^2$  up to  $z = 1$ . We find a detection significance for the total relativistic wide-angle effects that ranges from  $\sim 5\sigma$  to  $> 15\sigma$ , depending on the line-of-sight configuration.

---

## Contents

<b>1</b>	<b>Introduction</b>	<b>1</b>
<b>2</b>	<b>Relativistic and wide-angle corrections in the number counts</b>	<b>2</b>
<b>3</b>	<b>Auto- and cross-power spectra</b>	<b>5</b>
<b>4</b>	<b>Illustrating the relativistic and wide-angle effects</b>	<b>7</b>
<b>5</b>	<b>Detecting the relativistic and wide-angle effects</b>	<b>9</b>
<b>6</b>	<b>Conclusions</b>	<b>15</b>
<b>A</b>	<b>Fourier kernels</b>	<b>17</b>
<b>B</b>	<b>Coefficients <math>C_{lmn}^{(ab)}</math></b>	<b>18</b>
<b>C</b>	<b>Multipoles of the power spectra</b>	<b>20</b>

---

## 1 Introduction

The dark matter density contrast can be traced by galaxies, allowing us to probe the Universe and thus test cosmological models and gravity itself. The underlying dark matter distribution imparts peculiar velocities to galaxies, which distort the galaxy positions along the line of sight. These redshift-space distortions are dominated by the Kaiser effect but also include further relativistic effects [1–4]. In a Fourier space analysis of redshift-space distortions, it is common to use the plane-parallel or flat-sky approximation in which the line-of-sight direction from an observer to different galaxy pairs is fixed.

For next-generation surveys with wide sky coverage, the flat-sky limit cannot be expected to deliver the necessary theoretical accuracy. In fact it is necessary for consistency to include the relativistic corrections with the wide-angle corrections – since they are of the same order of magnitude on ultra-large scales. Furthermore, these corrections can reinforce each other and can also partially cancel each other, depending on the properties of the tracers. A theoretically complete solution requires a full-sky analysis, using the 2-point correlation function or its angular harmonic (or spherical Fourier-Bessel) transform and including all wide-angle and relativistic contributions [3–8].<sup>1</sup> However this is computationally very intensive and a simpler approach is the approximate inclusion of leading-order wide-angle corrections to the plane-parallel limit (see e.g. [15–17]). Recent works have included relativistic effects in the wide-angle corrections of the galaxy power spectrum [18] and its multipoles [19–23].

A common approach to derive the wide-angle corrections to the Fourier power spectrum is to perturbatively compute the expansions of appropriate wide-angle terms in configuration space and then take the Fourier transform of the result [15, 16, 19, 23]. In this paper, we follow an alternative perturbative approach adopted by [22]. We generalise their result from the midpoint line of sight to all possible lines of sight. We include the standard redshift-space distortions and the non-integrated relativistic corrections from Doppler and Sachs-Wolfe effects,

---

<sup>1</sup>See e.g. [9–14] for earlier work on general wide-angle correlations, without including relativistic effects.

thereby generalising [23] which only considered the Doppler contribution. The integrated relativistic corrections from lensing magnification and time delay effects are included in the midpoint results of [22] but we omit these effects in our generalisation, leaving them for future work. We investigate the detectability of the relativistic, wide-angle and combined corrections by computing the  $\chi^2$  for two futuristic galaxy surveys and their cross power.

## 2 Relativistic and wide-angle corrections in the number counts

For a given source population  $a$ , the dominant terms in the redshift-space number density contrast at linear order are

$$\Delta_a(z, \mathbf{x}_a) = b_a(z)\delta(z, \mathbf{x}_a) - \frac{1}{\mathcal{H}(z)}\partial_{\parallel}^2 V(z, \mathbf{x}_a), \quad (2.1)$$

where  $|\mathbf{x}_a|$  is the comoving line-of-sight distance to redshift  $z$ ,  $b_a$  is the bias of tracer  $a$ ,  $\mathcal{H} = (1+z)^{-1}H = H_0[(1+z)^3\Omega_{m0} + 1 - \Omega_{m0}]^{1/2}$  is the conformal Hubble parameter,  $\delta$  is the matter density contrast,  $v_i = \partial_i V$  is the peculiar velocity, and  $\partial_{\parallel} = \hat{\mathbf{x}}_a \cdot \nabla$  is the derivative along the line of sight  $\hat{\mathbf{x}}_a$ . In Fourier space (2.1) is

$$\Delta_a(z, \mathbf{k}, \hat{\mathbf{x}}_a) = \left[ b_a(z) + f(z) (\hat{\mathbf{k}} \cdot \hat{\mathbf{x}}_a)^2 \right] \delta(z, \mathbf{k}), \quad (2.2)$$

where  $f = -d \ln D / d \ln(1+z)$  is the linear matter growth rate,  $D$  is the growth factor (normalized to 1 today), and we used the continuity equation  $V = -(\mathcal{H}/k^2) f \delta$ .

First, we consider the non-integrated relativistic corrections to the density contrast in (2.1), which are the Doppler (D) and gravitational potential ( $\Phi$ ) terms. In Newtonian gauge [4]:

$$\Delta_a^{\text{D}}(z, \mathbf{x}_a) = \left[ \mathcal{E}_a(z) - 2\mathcal{Q}_a(z) + \frac{2[\mathcal{Q}_a(z) - 1]}{x_a \mathcal{H}(z)} - \frac{\mathcal{H}(z)'}{\mathcal{H}(z)^2} \right] \partial_{\parallel} V(z, \mathbf{x}_a), \quad (2.3)$$

$$\begin{aligned} \Delta_a^{\Phi}(z, \mathbf{x}_a) &= \left[ -1 - \mathcal{E}_a(z) + 4\mathcal{Q}_a(z) - \frac{2[\mathcal{Q}_a(z) - 1]}{x_a \mathcal{H}(z)} + \frac{\mathcal{H}(z)'}{\mathcal{H}(z)^2} \right] \Phi(z, \mathbf{x}_a) \\ &+ \frac{1}{\mathcal{H}(z)} \Phi'(z, \mathbf{x}_a) + (3 - \mathcal{E}_a) \mathcal{H}(z) V(z, \mathbf{x}_a), \end{aligned} \quad (2.4)$$

where  $\Phi = -(3/2)\Omega_m(\mathcal{H}/k)^2\delta$  by the Poisson equation. Here  $\mathcal{E}$  (which is often denoted  $b_e$  or  $f_{\text{evo}}$ ) and  $\mathcal{Q}$  ( $= 5s/2$ ) are the evolution and magnification biases (see e.g. [24]):

$$\mathcal{E}_a = -\frac{\partial \ln n_a}{\partial \ln(1+z)}, \quad \mathcal{Q}_a = -\frac{\partial \ln n_a}{\partial \ln L_{c,a}}, \quad (2.5)$$

where  $n_a$  is the background comoving number density of sample  $a$  and  $L_{c,a}$  is the luminosity cut of the sources detected, given the specifications of the survey under consideration.

It is important to highlight the point that here  $\delta$  is the matter density contrast in comoving gauge. When we include ultra-large scale effects from relativistic or wide-angle corrections, it is advisable to use the comoving density contrast  $\delta$  [4, 25]. If this is not done, then two important relations above break down on ultra-large scales and need to be modified:

- (a) the scale-independent bias relation  $\delta_a(z, \mathbf{k}) = b_a(z) \delta(z, \mathbf{k})$ , and
- (b) the simple form of the Poisson equation,  $\nabla^2 \Phi \propto \delta$ .

In Fourier space, (2.3) and (2.4) may be written as

$$\Delta_a^{\text{D}} = i \frac{1}{k} \gamma_a^{\text{D}} (\hat{\mathbf{k}} \cdot \hat{\mathbf{x}}_a) \delta \quad \text{and} \quad \Delta_a^{\Phi} = \frac{1}{k^2} \gamma_a^{\Phi} \delta, \quad (2.6)$$

where

$$\gamma_a^{\text{D}} = \mathcal{H} f \left[ \mathcal{E}_a - 2\mathcal{Q}_a + \frac{2(\mathcal{Q}_a - 1)}{x_a \mathcal{H}} - \frac{\mathcal{H}'}{\mathcal{H}^2} \right], \quad (2.7)$$

$$\gamma_a^{\Phi} = \frac{3}{2} \Omega_m \mathcal{H}^2 \left[ 2 + \mathcal{E}_a - f - 4\mathcal{Q}_a + \frac{2(\mathcal{Q}_a - 1)}{x_a \mathcal{H}} - \frac{\mathcal{H}'}{\mathcal{H}^2} \right] + \mathcal{H}^2 f(3 - \mathcal{E}_a). \quad (2.8)$$

From now on, we will neglect terms that are of order  $\delta(\mathcal{H}/k)^n$ , where  $n > 2$ . For consistency, all terms with  $n \leq 2$  should be included.

The relativistic corrections are added to the density contrast in (2.2) to give

$$\begin{aligned} \Delta_a(z, \mathbf{k}, \hat{\mathbf{x}}_a) &= \left[ b_a(z) + f(z) (\hat{\mathbf{k}} \cdot \hat{\mathbf{x}}_a)^2 + i \frac{1}{k} \gamma_a^{\text{D}}(z) (\hat{\mathbf{k}} \cdot \hat{\mathbf{x}}_a) + \frac{1}{k^2} \gamma_a^{\Phi}(z) \right] \delta(z, \mathbf{k}) \\ &= \mathcal{K}_a(z, \mathbf{k}, \hat{\mathbf{x}}_a) \delta(z, \mathbf{k}), \end{aligned} \quad (2.9)$$

where  $\mathcal{K}_a$  is the total Fourier kernel for tracer  $a$ . Typically (2.9) is simplified using the plane-parallel approximation. However, the inclusion of relativistic corrections naturally requires the additional inclusion of wide-angle corrections, which are of the same parametric order, i.e.  $O[\delta(\mathcal{H}/k)]$ . In order to implement wide-angle corrections, we need to specify the geometric set-up.

We choose a line-of-sight vector  $\mathbf{r}$  from the observer to the separation vector  $\mathbf{x}_{ab} = \mathbf{x}_a - \mathbf{x}_b$  (see Figure 1):

$$\mathbf{x}_a = \mathbf{r} - (1-t) \mathbf{x}_{ab} \quad \text{and} \quad \mathbf{x}_b = \mathbf{r} + t \mathbf{x}_{ab}, \quad (2.10)$$

where  $0 \leq t \leq 1$ . The endpoint ( $t = 0$  or  $1$ ) and midpoint ( $t = 1/2$ ) are typical choices.

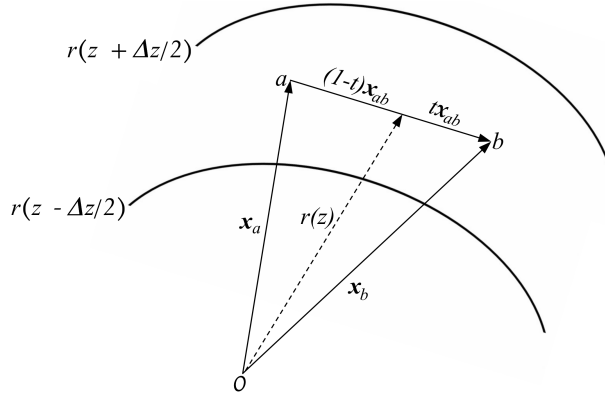


**Figure 1.** Geometry of the two-point correlation function for a pair of fluctuations.

Then we define the perturbation parameter vector [22]

$$\boldsymbol{\epsilon} = \frac{\mathbf{x}_{ab}}{r}, \quad (2.11)$$

which requires that the galaxy separation is less than the line-of-sight distance, i.e.,  $x_{ab} < r$  (see [17] for a detailed discussion of the validity of the perturbative wide-angle expansion). In Fourier space,  $x_{ab} < r$  imposes a minimum  $k_\epsilon(z)$  for the validity of the perturbative expansion:

$$k > k_\epsilon(z) = \frac{1}{r(z)}. \quad (2.12)$$

We follow [22] in neglecting the radial variations in a redshift bin, effectively treating all quantities in a bin as at the mid-redshift. See [23] for the inclusion of the radial corrections.

We rewrite (2.10) as

$$\mathbf{x}_a = [\hat{\mathbf{r}} - (1-t)\boldsymbol{\epsilon}]r \quad \text{and} \quad \mathbf{x}_b = (\hat{\mathbf{r}} + t\boldsymbol{\epsilon})r. \quad (2.13)$$

Taking the products  $\mathbf{x}_a \cdot \mathbf{x}_a$ , it follows that

$$\frac{1}{x_a} = \frac{1}{r} \left[ 1 + (1-t)(\boldsymbol{\epsilon} \cdot \hat{\mathbf{r}}) + \frac{3}{2}(1-t)^2(\boldsymbol{\epsilon} \cdot \hat{\mathbf{r}})^2 - \frac{1}{2}(1-t)^2\epsilon^2 \right], \quad (2.14)$$

$$\frac{1}{x_b} = \frac{1}{r} \left[ 1 - t(\boldsymbol{\epsilon} \cdot \hat{\mathbf{r}}) + \frac{3}{2}t^2(\boldsymbol{\epsilon} \cdot \hat{\mathbf{r}})^2 - \frac{1}{2}t^2\epsilon^2 \right], \quad (2.15)$$

where we keep terms up to  $O(\epsilon^2)$ . Using the above results in (2.13), we obtain

$$\hat{\mathbf{x}}_a = \left[ 1 + (1-t)(\boldsymbol{\epsilon} \cdot \hat{\mathbf{r}}) + \frac{3}{2}(1-t)^2(\boldsymbol{\epsilon} \cdot \hat{\mathbf{r}})^2 - \frac{1}{2}(1-t)^2\epsilon^2 \right] \hat{\mathbf{r}} - (1-t)[1 + (1-t)(\boldsymbol{\epsilon} \cdot \hat{\mathbf{r}})]\boldsymbol{\epsilon}, \quad (2.16)$$

$$\hat{\mathbf{x}}_b = \left[ 1 - t(\boldsymbol{\epsilon} \cdot \hat{\mathbf{r}}) + \frac{3}{2}t^2(\boldsymbol{\epsilon} \cdot \hat{\mathbf{r}})^2 - \frac{1}{2}t^2\epsilon^2 \right] \hat{\mathbf{r}} + t[1 - t(\boldsymbol{\epsilon} \cdot \hat{\mathbf{r}})]\boldsymbol{\epsilon}. \quad (2.17)$$

We decompose  $\mathbf{k}$  and  $\boldsymbol{\epsilon}$  into their Cartesian components  $(k_x, k_y, k_z)$ , taking the  $z$ -axis to be along the line of sight  $\mathbf{r}$  to redshift  $z$ . Then using (2.16) and (2.17), we can write the total Fourier kernel given in (2.9) as

$$\mathcal{K}_a = \mathcal{K}_a^{\text{S}} + \mathcal{K}_a^{\text{R}} + \mathcal{K}_a^{\text{W}} + \mathcal{K}_a^{\text{RW}}, \quad (2.18)$$

where the  $\mathcal{K}_a^{\text{I}}$  are as follows.

- S: The standard Newtonian plane-parallel Kaiser part:

$$\mathcal{K}_a^{\text{S}} = b_a + f \left( \frac{k_z}{k} \right)^2 \quad \text{where} \quad k_z = \mathbf{k} \cdot \hat{\mathbf{r}} \equiv \mu k. \quad (2.19)$$

- R: The plane-parallel relativistic corrections to the standard kernel:

$$\mathcal{K}_a^{\text{R}} = \mathcal{K}_a^{\text{D}} + \mathcal{K}_a^{\Phi}, \quad \text{where} \quad \mathcal{K}_a^{\text{D}} = i \frac{k_z}{k} \gamma_a^{\text{D}}, \quad \mathcal{K}_a^{\Phi} = \frac{1}{k^2} \gamma_a^{\Phi}. \quad (2.20)$$

- W: The Newtonian wide-angle corrections to the standard kernel:

$$\mathcal{K}_a^{\text{W}}, \text{ given in Appendix A.}$$

- RW: The wide-angle corrections to the plane-parallel relativistic kernel:

$$\mathcal{K}_a^{\text{RW}}, \text{ given in Appendix A.}$$

Then the full kernel, i.e. standard + combined relativistic wide-angle correction is

$$\mathcal{K}_a = \mathcal{K}_a^{\text{S}} + \mathcal{K}_a^{\text{W}} + \mathcal{K}_a^{\text{R}} + \mathcal{K}_a^{\text{RW}}. \quad (2.21)$$

### 3 Auto- and cross-power spectra

The Fourier power spectra are

$$P_{ab}(\mathbf{k}, \mathbf{r}) = \int \frac{d^3 \mathbf{k}'}{(2\pi)^3} \int d^3 \boldsymbol{\epsilon} r e^{-i\mathbf{r}(\mathbf{k}-\mathbf{k}')\cdot\boldsymbol{\epsilon}} \mathcal{K}_a(\mathbf{k}', \boldsymbol{\epsilon}, \mathbf{r}) \mathcal{K}_b^*(\mathbf{k}', \boldsymbol{\epsilon}, \mathbf{r}) P(k'), \quad (3.1)$$

where  $P$  is the linear matter power spectrum and we omit the dependencies on  $z$  here and below for brevity. These are the ‘local’ power spectra, i.e. the Fourier power spectra at line-of-sight position  $\mathbf{r}(z)$ . The ‘full’ power spectra are then given by an integral over all lines of sight [22],

$$P_{ab}^{\text{full}}(\mathbf{k}) = \frac{1}{V_s} \int d^3 \mathbf{r} P_{ab}(\mathbf{k}, \mathbf{r}), \quad (3.2)$$

where  $V_s(z)$  is the survey volume. In this paper we will work with the local power spectra.

The product of Fourier kernels in (3.1) can be written in the form [22]:

$$\mathcal{K}_a(\mathbf{k}', \boldsymbol{\epsilon}, \mathbf{r}) \mathcal{K}_b^*(\mathbf{k}', \boldsymbol{\epsilon}, \mathbf{r}) = \sum_{l,m,n} \mathcal{C}_{lmn}^{(ab)}(\mathbf{k}', \mathbf{r}) \epsilon_x^l \epsilon_y^m \epsilon_z^n, \quad (3.3)$$

where the coefficients  $\mathcal{C}_{lmn}^{(ab)}$  are independent of  $\boldsymbol{\epsilon}$  and where  $l + m + n \leq 2$ , since we expand up to  $\epsilon^2$ . Then the power spectrum (3.1) becomes

$$P_{ab}(\mathbf{k}, \mathbf{r}) = \sum_{l,m,n} \int \frac{d^3 \mathbf{k}'}{(2\pi)^3} \int d^3 \mathbf{x}_{ab} e^{-i(\mathbf{k}-\mathbf{k}')\cdot\mathbf{x}_{ab}} \epsilon_x^l \epsilon_y^m \epsilon_z^n \mathcal{C}_{lmn}^{(ab)}(\mathbf{k}', \mathbf{r}) P(k'), \quad (3.4)$$

where  $r d^3 \boldsymbol{\epsilon} = d^3 \mathbf{x}_{ab}$  from (2.11). The useful relation

$$e^{-i(\mathbf{k}-\mathbf{k}')\cdot\mathbf{x}_{ab}} \epsilon_x^l \epsilon_y^m \epsilon_z^n = \left(\frac{-i}{r}\right)^{l+m+n} \left(\frac{\partial}{\partial k'_x}\right)^l \left(\frac{\partial}{\partial k'_y}\right)^m \left(\frac{\partial}{\partial k'_z}\right)^n [e^{-i(\mathbf{k}-\mathbf{k}')\cdot\mathbf{x}_{ab}}], \quad (3.5)$$

leads to

$$P_{ab} = \sum_{l,m,n} \left(\frac{-i}{r}\right)^{l+m+n} \int \frac{d^3 \mathbf{k}'}{(2\pi)^3} I_{lmn}^{(ab)}, \quad (3.6)$$

where

$$I_{lmn}^{(ab)} = \mathcal{C}_{lmn}^{(ab)} P \left(\frac{\partial}{\partial k'_x}\right)^l \left(\frac{\partial}{\partial k'_y}\right)^m \left(\frac{\partial}{\partial k'_z}\right)^n \int d^3 \mathbf{x}_{ab} e^{-i(\mathbf{k}-\mathbf{k}')\cdot\mathbf{x}_{ab}}. \quad (3.7)$$

Here we moved the  $\boldsymbol{\epsilon}$ -independent coefficients and derivative operators out of the  $\mathbf{x}_{ab}$  integral, which gives the 3D Dirac-delta function:

$$\int d^3 \mathbf{x}_{ab} e^{i(\mathbf{k}'-\mathbf{k})\cdot\mathbf{x}_{ab}} = (2\pi)^3 \delta^{\text{Dirac}}(\mathbf{k}' - \mathbf{k}). \quad (3.8)$$

Using the identity

$$\int dx f(x) \frac{\partial^q}{\partial x^q} [\delta^{\text{Dirac}}(x - x_0)] = (-1)^q \frac{\partial^q}{\partial x^q} f(x) \Big|_{x=x_0}, \quad (3.9)$$

we find that

$$\begin{aligned}
P_{ab} &= \sum_{l,m,n} \left(\frac{i}{r}\right)^{l+m+n} \left(\frac{\partial}{\partial k'_x}\right)^l \left(\frac{\partial}{\partial k'_y}\right)^m \left(\frac{\partial}{\partial k'_z}\right)^n \left[\mathcal{C}_{lmn}^{(ab)} P\right] \\
&= P_{ab}^S + P_{ab}^R + P_{ab}^W + P_{ab}^{RW} + O[\epsilon^3, \delta(\mathcal{H}/k)^3] .
\end{aligned} \tag{3.10}$$

The non-vanishing coefficients  $\mathcal{C}_{lmn}^{(ab)}$  in (3.10) are given in [Appendix B](#) and the individual spectra on the right of (3.10) are as follows:

$$P_{ab}^S = \mathcal{K}_a^S \mathcal{K}_b^S P , \tag{3.11}$$

$$P_{ab}^R = \left[ \mathcal{K}_a^S \mathcal{K}_b^{D*} + \mathcal{K}_b^S \mathcal{K}_a^D + \mathcal{K}_a^S \mathcal{K}_b^\Phi + \mathcal{K}_b^S \mathcal{K}_a^\Phi + \mathcal{K}_a^D \mathcal{K}_b^{D*} \right] P , \tag{3.12}$$

together with

$$\begin{aligned}
P_{ab}^W &= \frac{1}{(kr)^2} f \left\{ 8t(1-t)f\mu^2[1 + 2\mu^2(-5 + 6\mu^2)] \right. \\
&\quad + 2\mu^2(-7 + 10\mu^2) \left[ t^2 k \partial_k \mathcal{K}_a^S + (1-t)^2 k \partial_k \mathcal{K}_b^S \right] \\
&\quad + 4\mu^3 \left[ t^2 k \partial_{k_z} \mathcal{K}_a^S + (1-t)^2 k \partial_{k_z} \mathcal{K}_b^S \right] \\
&\quad + (1-\mu^2)(-1 + 4\mu^2) \left[ t^2 k^2 \partial_k^2 \mathcal{K}_a^S + (1-t)^2 k^2 \partial_k^2 \mathcal{K}_b^S \right] \\
&\quad \left. + 2(1-\mu^2)\mu \left[ t^2 k^2 \partial_{k_z} \partial_k \mathcal{K}_a^S + (1-t)^2 k^2 \partial_{k_z} \partial_k \mathcal{K}_b^S \right] \right\} P \\
&+ i \frac{2}{kr} f \mu \left\{ 2\mu^2 \left[ t \mathcal{K}_a^S - (1-t) \mathcal{K}_b^S \right] \right. \\
&\quad \left. + (1-\mu^2) \left[ t k \partial_k \mathcal{K}_a^S - (1-t) k \partial_k \mathcal{K}_b^S \right] \right\} P \\
&+ \frac{2}{(kr)^2} f \left\{ 2t(1-t)f\mu^2(1-\mu^2)(-2 + 9\mu^2) \right. \\
&\quad + \mu^2(-7 + 10\mu^2) \left[ t^2 \mathcal{K}_a^S + (1-t)^2 \mathcal{K}_b^S \right] \\
&\quad + (1-\mu^2)(-1 + 4\mu^2) \left[ t^2 k \partial_k \mathcal{K}_a^S + (1-t)^2 k \partial_k \mathcal{K}_b^S \right] \\
&\quad \left. + (1-\mu^2)\mu \left[ t^2 k \partial_{k_z} \mathcal{K}_a^S + (1-t)^2 k \partial_{k_z} \mathcal{K}_b^S \right] \right\} k \partial_k P \\
&+ i \frac{2}{kr} f \mu (1-\mu^2) \left[ t \mathcal{K}_a^S - (1-t) \mathcal{K}_b^S \right] k \partial_k P \\
&+ \frac{1}{(kr)^2} f (1-\mu^2) \left\{ 4t(1-t)f\mu^2(1-\mu^2) \right. \\
&\quad \left. + (-1 + 4\mu^2) \left[ t^2 \mathcal{K}_a^S + (1-t)^2 \mathcal{K}_b^S \right] \right\} k^2 \partial_k^2 P ,
\end{aligned} \tag{3.13}$$

and

$$\begin{aligned}
P_{ab}^{\text{RW}} = & f \left\{ -\frac{1}{kr} \frac{\mathcal{H}}{k} \left\{ 2\mu^2 \left[ t \left( 2\mathcal{Q}_b - \mathcal{E}_b + \frac{\mathcal{H}'}{\mathcal{H}^2} \right) \mathcal{K}_a^{\text{S}} + (1-t) \left( 2\mathcal{Q}_a - \mathcal{E}_a + \frac{\mathcal{H}'}{\mathcal{H}^2} \right) \mathcal{K}_b^{\text{S}} \right] \right. \right. \\
& + (1-\mu^2) \left[ t \left( 2\mathcal{Q}_b - \mathcal{E}_b + \frac{\mathcal{H}'}{\mathcal{H}^2} \right) k \partial_k \mathcal{K}_a^{\text{S}} + (1-t) \left( 2\mathcal{Q}_a - \mathcal{E}_a + \frac{\mathcal{H}'}{\mathcal{H}^2} \right) k \partial_k \mathcal{K}_b^{\text{S}} \right] \left. \right\} \\
& + \frac{2}{(kr)^2} \left\{ (1-4\mu^2) \left[ t(1-\mathcal{Q}_b) \mathcal{K}_a^{\text{S}} + (1-t)(1-\mathcal{Q}_a) \mathcal{K}_b^{\text{S}} \right] \right. \\
& \quad + (2\mu^2-1) \left[ t(1-\mathcal{Q}_b) k \partial_k \mathcal{K}_a^{\text{S}} + (1-t)(1-\mathcal{Q}_a) k \partial_k \mathcal{K}_b^{\text{S}} \right] \\
& \quad \left. + \mu \left[ t(1-\mathcal{Q}_b) k \partial_{k_z} \mathcal{K}_a^{\text{S}} + (1-t)(1-\mathcal{Q}_a) k \partial_{k_z} \mathcal{K}_b^{\text{S}} \right] \right\} \\
& + i \frac{2}{kr} \mu \left\{ 2\mu^2 \left[ t \mathcal{K}_a^{\text{D}} - (1-t) \mathcal{K}_b^{\text{D}*} \right] \right. \\
& \quad \left. + (1-\mu^2) \left[ t k \partial_k \mathcal{K}_a^{\text{D}} - (1-t) k \partial_k \mathcal{K}_b^{\text{D}*} \right] \right\} \left. \right\} P \\
& + f \left\{ \frac{1}{kr} \frac{\mathcal{H}}{k} (\mu^2-1) \left[ t \left( 2\mathcal{Q}_b - \mathcal{E}_b + \frac{\mathcal{H}'}{\mathcal{H}^2} \right) \mathcal{K}_a^{\text{S}} + (1-t) \left( 2\mathcal{Q}_a - \mathcal{E}_a + \frac{\mathcal{H}'}{\mathcal{H}^2} \right) \mathcal{K}_b^{\text{S}} \right] \right. \\
& \quad + \frac{2}{(kr)^2} (2\mu^2-1) \left[ t(1-\mathcal{Q}_b) \mathcal{K}_a^{\text{S}} + (1-t)(1-\mathcal{Q}_a) \mathcal{K}_b^{\text{S}} \right] \\
& \quad \left. + i \frac{2}{kr} \mu (1-\mu^2) \left[ t \mathcal{K}_a^{\text{D}} - (1-t) \mathcal{K}_b^{\text{D}*} \right] \right\} k \partial_k P \\
& + \frac{1}{(kr)^2} f (1-\mu^2) \left\{ 4t(1-t) f \mu^2 (1-\mu^2) \right. \\
& \quad \left. + (4\mu^2-1) \left[ t^2 \mathcal{K}_a^{\text{S}} + (1-t)^2 \mathcal{K}_b^{\text{S}} \right] \right\} k^2 \partial_k^2 P. \tag{3.14}
\end{aligned}$$

Note that in the expressions (3.13) and (3.14), there are real terms with a factor of  $\mu \partial_{k_z} \mathcal{K}_a^{\text{S}}$  or  $\mu \partial_{k_z} \partial_k \mathcal{K}_a^{\text{S}}$ , which appear to be terms multiplied by an odd power of  $\mu$ . However the  $k_z$  derivative introduces another factor of  $\mu = k_z/k$ , as can be seen in (A.5) and (A.6), so that these terms are indeed even in  $\mu$ .

The multipoles of the power spectra are given by

$$P_{ab}^{\text{I}(\ell)}(k) = \frac{(2\ell+1)}{2} \int_{-1}^{+1} d\mu P_{ab}^{\text{I}}(k, \mu) \mathcal{L}_\ell(\mu) \quad \text{where I = S, R, W, RW or R+W+RW.} \tag{3.15}$$

Detailed expressions for  $\ell = 0, 1, 2$  are given in [Appendix C](#).

#### 4 Illustrating the relativistic and wide-angle effects

In order to illustrate the relativistic and wide-angle effects, we need examples of galaxy samples. For each sample we require the clustering, evolution and magnification biases, together with the number densities. It is important that these quantities are *physically self-consistent*. This is achieved by using clustering biases  $b_a$  that are based on simulations or a halo model, and by deriving  $\mathcal{E}_a$ ,  $\mathcal{Q}_a$  and  $n_a$  from a physically motivated luminosity function. To this end, we adapt the models described in [24] to the following futuristic mock samples:



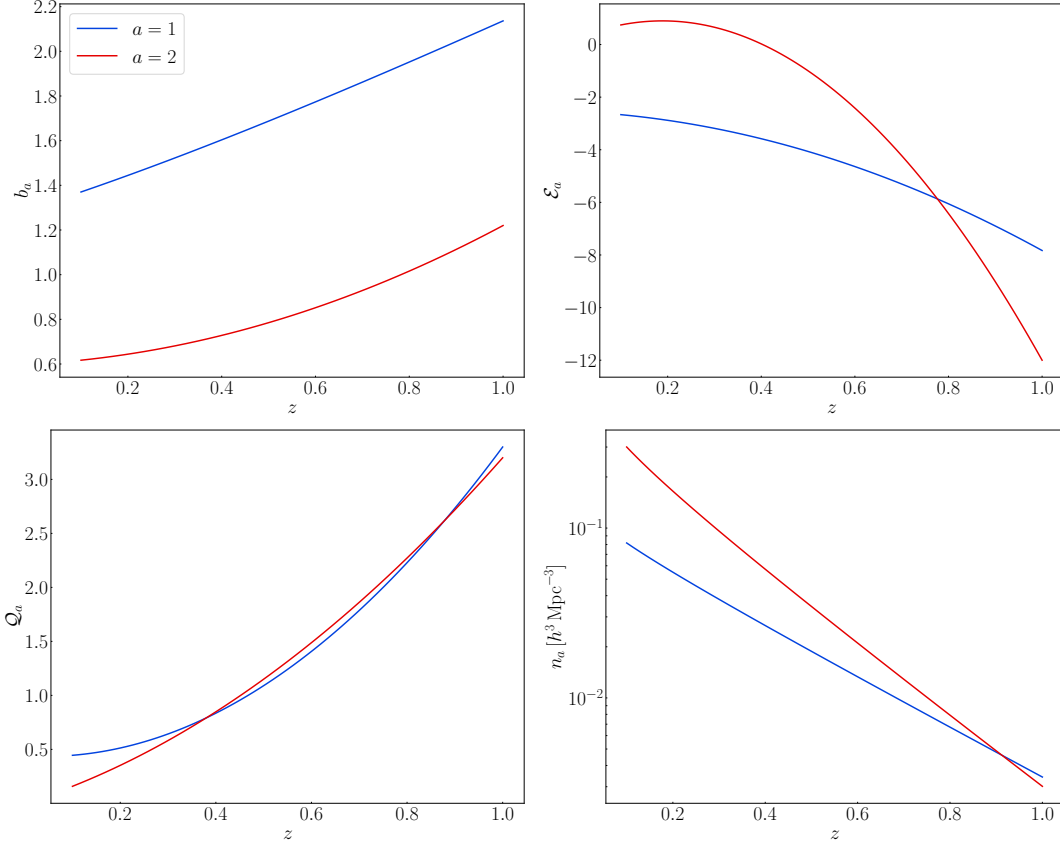


**Figure 2.** Clustering bias (*top left*), evolution bias (*top right*), magnification bias (*bottom left*) and number density (*bottom right*) for the 2 futuristic galaxy samples, where  $a = 1$  is ‘beyond-DESI’ and  $a = 2$  is SKA Phase 2.

- $a = 1$ : a futuristic ‘beyond-DESI’ BGS sample with a fainter magnitude cut,  $m_c = 22$ .
- $a = 2$ : a futuristic SKA Phase 2 HI galaxy sample with flux density cut  $S_c = 5 \mu\text{Jy}$ .

For the clustering biases  $b_a$  ( $a = 1, 2$ ) we use [24]:

$$b_1 = \frac{1.3}{D(z)}, \quad b_2 = 0.60 + 0.12z + 0.50z^2. \quad (4.1)$$

We apply the futuristic flux cuts,  $m_c = 22$  (for  $a = 1$ ) and  $S_c = 5 \mu\text{Jy}$  (for  $a = 2$ ), to the luminosity function models in [24]. Then we find simple fits to the results:

$$\mathcal{E}_1 = -2.54 - 0.81z - 4.48z^2, \quad \mathcal{E}_2 = 0.2 + 7.4z - 19.6z^2, \quad (4.2)$$

$$\mathcal{Q}_1 = 0.44 - 0.26z + 3.12z^2, \quad \mathcal{Q}_2 = 1.4z + 1.8z^2, \quad (4.3)$$

$$n_1 = 0.09z^{-0.10} \exp(-3.27z) h^3 \text{Mpc}^{-3}, \quad n_2 = 0.3z^{-0.2} \exp(-4.6z) h^3 \text{Mpc}^{-3}. \quad (4.4)$$

For the redshift range and sky area, we assume

$$0.1 \leq z \leq 1, \quad \Omega_{\text{sky}} = 15\,000 \text{ deg}^2. \quad (4.5)$$

The biases  $b_a, \mathcal{E}_a, \mathcal{Q}_a$  and number densities  $n_a$  are presented in [Figure 2](#).

Examples of the monopole and dipole of the power spectra for these galaxy samples are shown in Figure 3 and Figure 4. Figure 5 presents the cross-power dipole for a different pair of tracers, i.e. 21cm intensity mapping (SKA-like) and H $\alpha$  galaxies (Euclid-like), at redshift  $z = 1$ . This further illustrates the large variety in the relativistic and wide-angle effects for different tracers. Note that the leading order relativistic contributions to the dipole do not depend on the line of sight. Furthermore, Figure 5 shows that the neglect of radial redshift derivatives can lead to non-negligible changes in signal, as shown in the (W + R) ratio for the  $t = 0$  case. (See [23] for more details.)

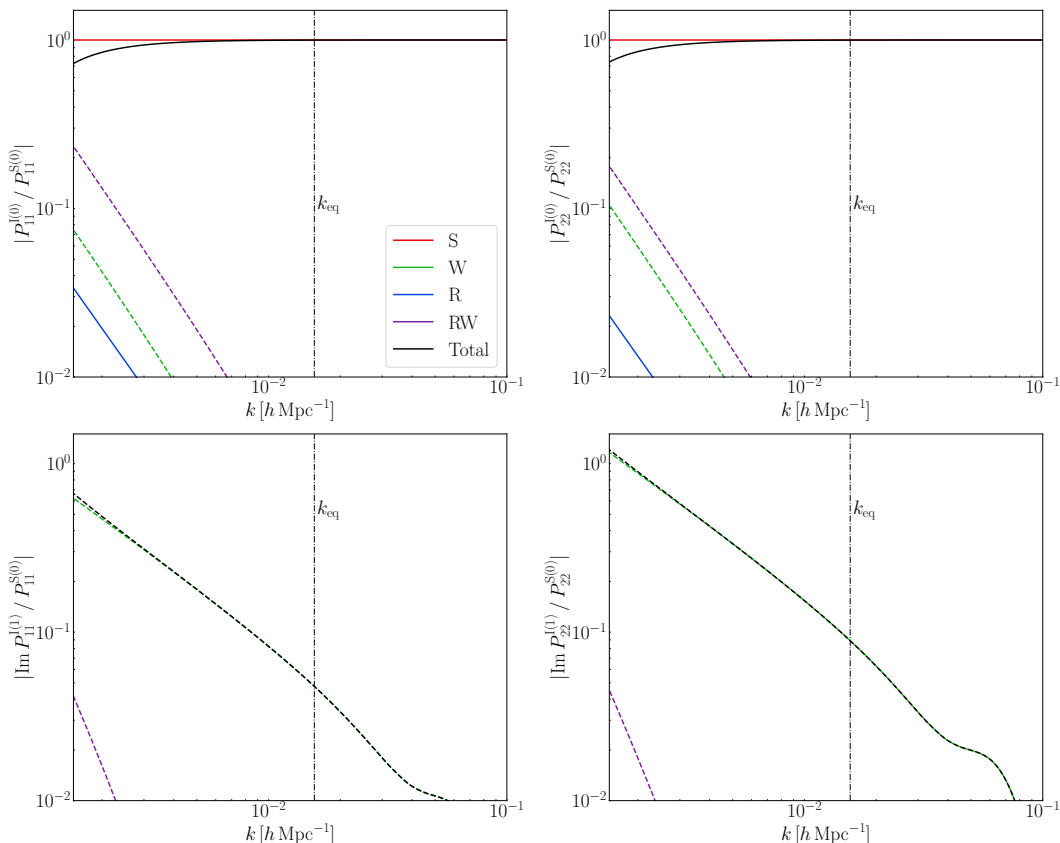


**Figure 3.** For the auto-power, the fractional correction to the standard monopole (*top row*) and the dipole relative to the standard monopole (*bottom row*), at  $z = 0.5$ . Galaxy samples are  $a = 1$  (*left*) and  $a = 2$  (*right*). The line of sight is endpoint,  $t = 0$ . Dashed lines indicate negative values.

## 5 Detecting the relativistic and wide-angle effects

Our aim is to test whether the detection of relativistic and wide-angle effects is feasible in futuristic galaxy surveys. Following [26], we compute the  $\chi^2$  values between the model  $P_{ab}^S + P_{ab}^I$ , which includes the relativistic and/or wide-angle effect I, and the standard model  $P_{ab}^S$ , which excludes the effect I. We consider all the cases of  $P_{ab}^I$ , where I=W, R, RW or W+R+RW. Our aim is to estimate the statistical significance of measuring effect I, against the null hypothesis of the absence of such an effect in the data. In our case, we use synthetic data generated by taking the theoretical prediction of the full power spectrum (3.10). Therefore

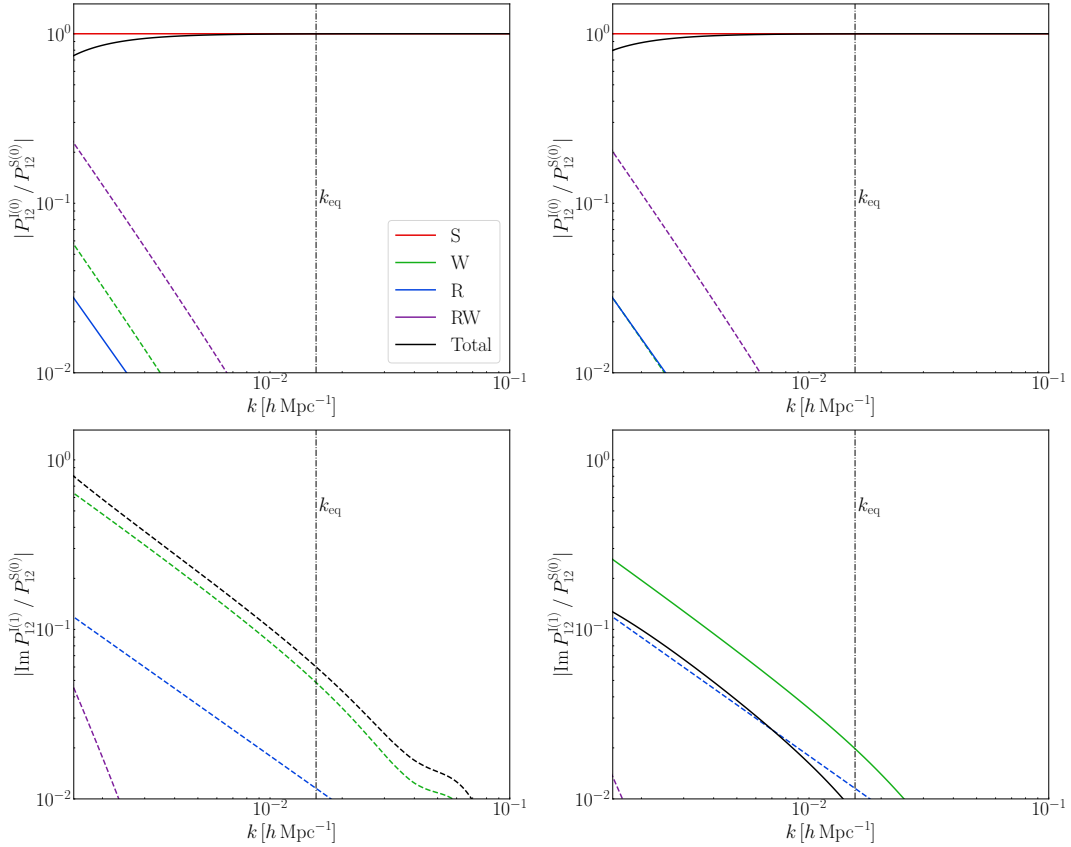


**Figure 4.** As in [Figure 3](#), for the cross-power between samples  $a = 1$  and  $2$ . Two configurations are shown: endpoint ( $t = 0$ , *left*) and midpoint ( $t = 0.5$ , *right*).

the  $\chi^2$  for effect I in a redshift bin centred at  $z_i$  is simply

$$\chi^2(z_i)^{\text{I}} = \sum_{k,\mu} \frac{|P_{ab}^{\text{I}}(z_i, k, \mu)|^2}{\text{Var}[P_{ab}(z_i, k, \mu)]}, \quad (5.1)$$

where the variance is given by

$$\text{Var}[P_{aa}] = \frac{2}{N_{\mathbf{k}}} |\tilde{P}_{aa}|^2, \quad \text{Var}[P_{12}] = \frac{1}{N_{\mathbf{k}}} \left[ |\tilde{P}_{12}|^2 + |\tilde{P}_{11}| |\tilde{P}_{22}| \right], \quad (5.2)$$

with

$$\tilde{P}_{ab} = P_{ab} + \frac{\delta_{ab}^{\text{Kronecker}}}{n_a} \quad \text{and} \quad P_{ab} = P_{ab}^{\text{S}} + P_{ab}^{\text{R+W+RW}}. \quad (5.3)$$

Note that  $P_{ab}$  in the variance in (5.1)–(5.2) is given by (3.10) – i.e. it includes *all* relativistic and wide-angle effects. The number of Fourier modes is

$$N_{\mathbf{k}} = \frac{2\pi k^2 \Delta k \Delta \mu}{k_{\text{f}}^3}, \quad (5.4)$$

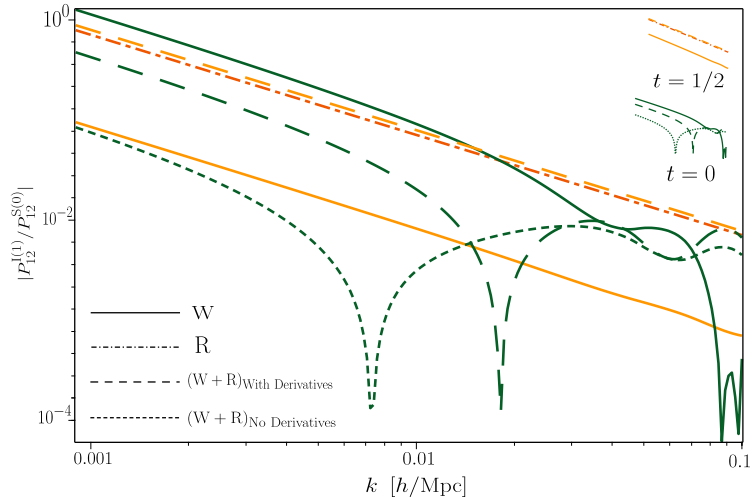


**Figure 5.** Imaginary part of the cross-power dipole (which is the main contributor in the imaginary part of the cross-power) as a fraction of the standard cross-power monopole. Here we use a different pair of tracers: tracer 1 is a SKA-like 21cm intensity mapping survey, while tracer 2 is a Euclid-like spectroscopic  $H\alpha$  survey. The redshift is  $z = 1$ . The relativistic (R, red) curve is for both lines of sight, since R is independent of  $t$ . The long-dashed curves show the wide-angle + relativistic (W+R) corrections, including the radial derivative corrections, as in [23]. For  $t = 0$ , we show also the curves when the radial derivatives are neglected (short-dashed curve), as in the main results of this paper.

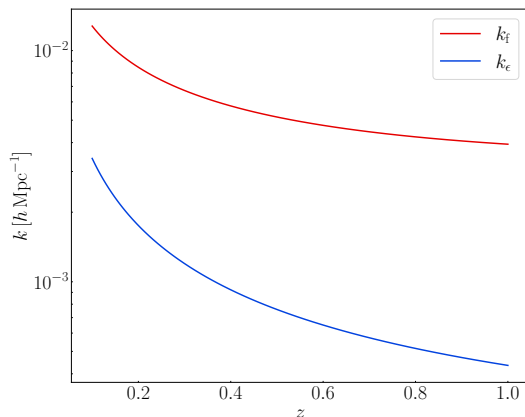


**Figure 6.** Longest wavelength modes in (5.8).

where the fundamental mode,  $k_f$ , corresponds to the longest wavelength that can be measured in the redshift bin. The  $\chi^2$  cumulative over redshift bins is

$$\chi^2(\leq z_i)^I = \sum_{j=1}^i \chi^2(z_j)^I. \quad (5.5)$$

The detection significance for effect I can be estimated as

$$\mathcal{S}(z_i)^I = \left[ \chi^2(z_i)^I \right]^{1/2}, \quad (5.6)$$

and similarly for the cumulative  $\mathcal{S}(\leq z_i)$ <sup>1</sup>.

For the numerical calculation we choose

$$\Delta z = 0.1, \quad \Delta\mu = 0.04, \quad \Delta k = k_f, \quad k_{\max} = 0.08(1+z)^{2/(2+n_s)} \text{ h Mpc}^{-1}. \quad (5.7)$$

The conservative choice of  $k_{\max}$  in (5.7) means that linear perturbations remain accurate. The minimum  $k$  in each redshift bin, corresponding to the longest wavelength mode, is given by

$$k_{\min}(z) = \max[k_f(z), k_\epsilon(z)], \quad (5.8)$$

where  $k_\epsilon$  is given in (2.12). These wavenumbers are shown in Figure 6, confirming that  $k_{\min} = k_f$  in the case of the two futuristic surveys over redshifts  $z \leq 1$  and sky area 15 000 deg<sup>2</sup>.

In the cases  $t = 0$  (endpoint) and  $t = 0.5$  (midpoint), the results for the detection significance  $\mathcal{S}$  are summarised in Figure 7 (per redshift) and Figure 8 (cumulative). The significance is higher for the endpoint configuration, but in both cases, the cumulative significance is  $> 5\sigma$ . If we combine the signals from auto- and cross-power, the significance for the endpoint  $t = 0$  line of sight is  $> 10\sigma$ . We note that for the midpoint line of sight, only the cross-power has a cumulative detection significance  $> 5\sigma$ .

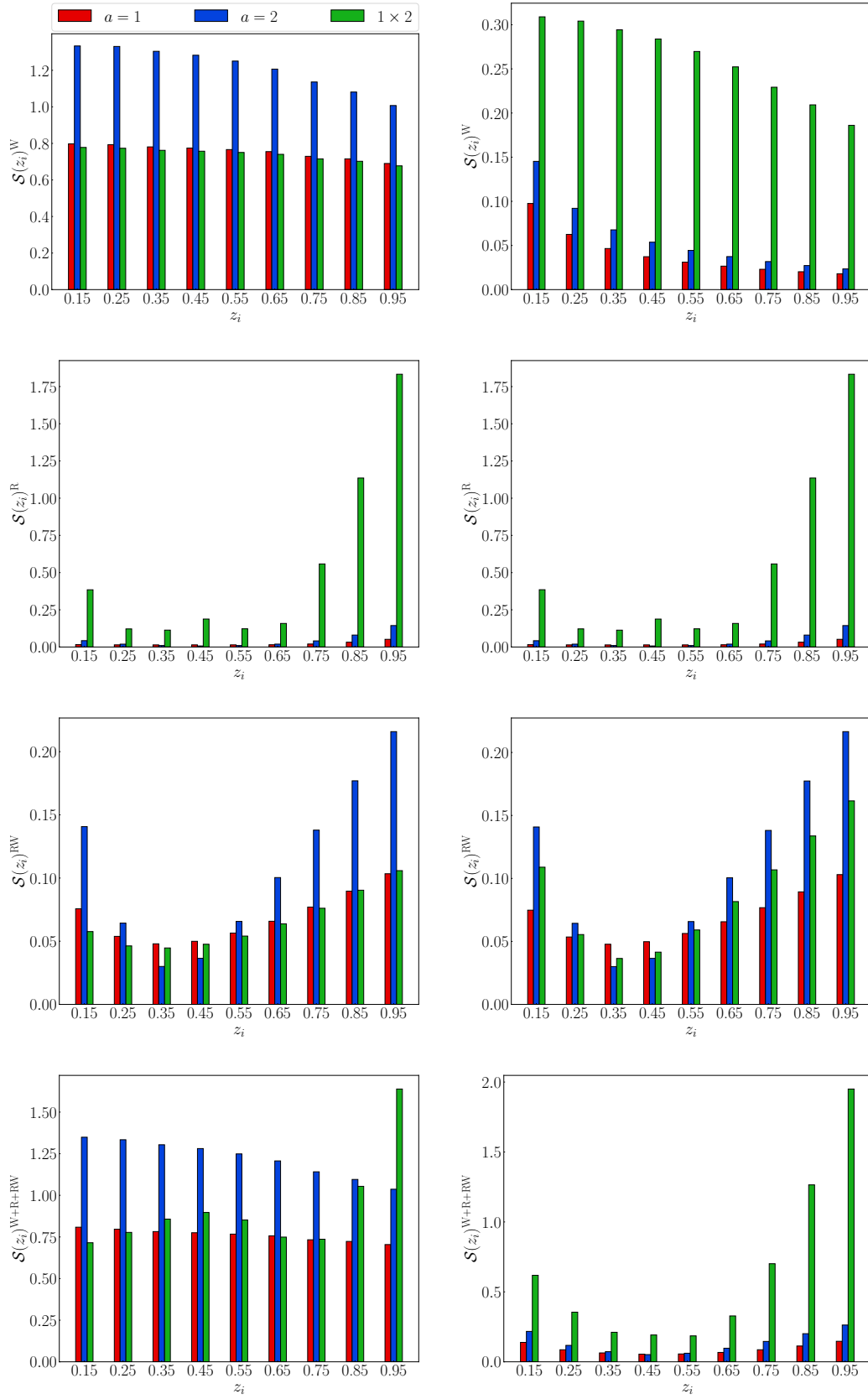


**Figure 7.** For the relativistic wide-angle power  $P_{ab}^I$ , where  $I=R, W, RW$  or  $R+W+RW$ , the detection significance  $\mathcal{S}^I$  is shown in the auto- and cross-power, in each  $z$ -bin, for the endpoint ( $t = 0$ , left) and midpoint ( $t = 0.5$ , right) lines of sight.

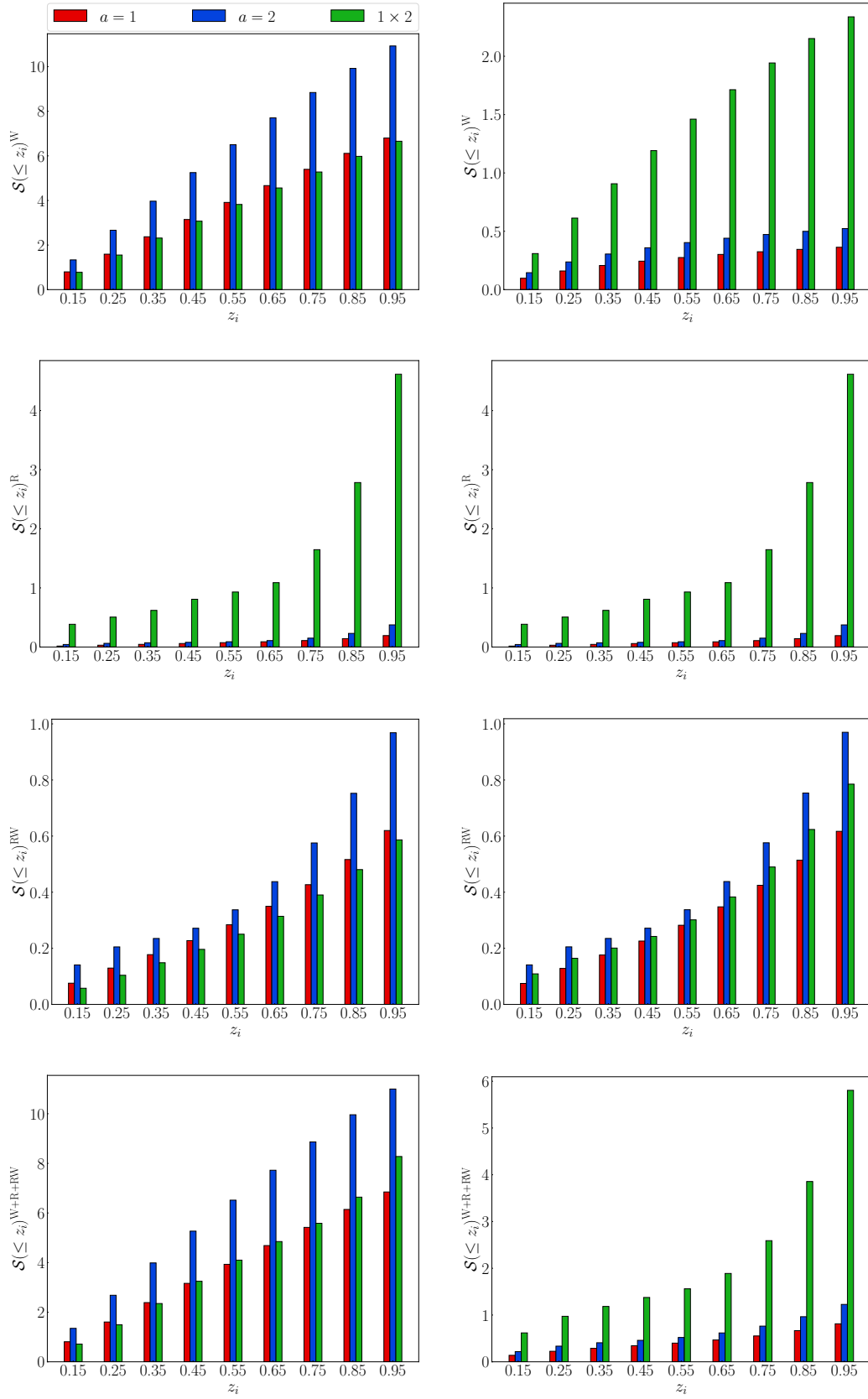


**Figure 8.** As in Figure 7, for the cumulative detection significance  $\mathcal{S}$  of the relativistic and wide-angle corrections in the auto- and cross-power, for the endpoint (*left*) and midpoint (*right*) lines of sight.

## 6 Conclusions

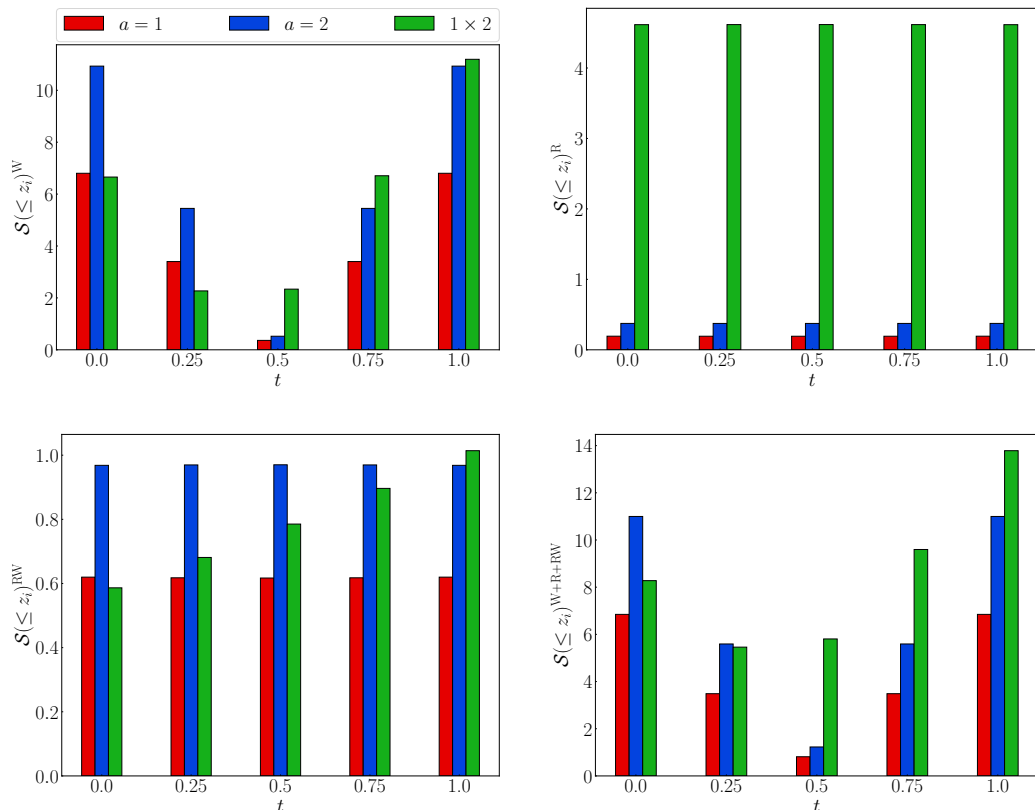


**Figure 9.** Cumulative detection significance  $\mathcal{S}$  of the relativistic and wide-angle corrections in the auto- and cross-power, against the line-of-sight parameter  $t$ .

This work complements the analysis presented in [22] by generalizing their power spectrum results to two tracers and to arbitrary lines of sight. We omit the integrated relativistic corrections – mainly the effect of lensing convergence – which should be reasonable at redshifts  $z < 1$ . The non-integrated relativistic effects in the auto-power are suppressed by a factor  $O[\delta(\mathcal{H}/k)^2]$ . In the imaginary part of the cross-power by contrast, there are terms  $O[\delta(\mathcal{H}/k)]$  [1, 26–34]. The consequent difference in signal is clearly apparent in the  $\mathcal{S}^R$  plots in Figure 7 and Figure 8. The pure relativistic contribution is insensitive to the line-of-sight parameter  $t$ , since it is computed in the plane-parallel approximation, as in (2.20). On the other hand, the wide-angle effects are obviously sensitive to  $t$ .

Both relativistic and wide-angle effects are very sensitive to the different astrophysical properties of the surveys. Nevertheless, Figure 7 and Figure 8 show that the cumulative R+W+RW signal is detectable in the cross-power at  $> 5\sigma$ . For  $t = 0$ , the signal is also detectable in the auto-power. In this case, the combined detection significance from cross- and auto-power is  $\sim 15\sigma$ .

What about other values of  $t$ ? Figure 9 shows how the detection significance varies across the full range of line-of-sight parameter  $t$ . In the case of the auto-power  $P_{aa}$ , there is a symmetry about  $t = 0.5$ , showing that the choice of a particular line of sight  $t$  is the mirror of  $1 - t$ . This symmetry is broken in the case of the cross-power  $P_{12}$ , because the permutation



of the tracers leads to different power spectra, as seen in the detailed forms (3.13) and (3.14). The results for the futuristic surveys indicate significant detection potential  $\sim 10\sigma$  for the cross-power  $P_{12}$  with  $t = 1$ , and for the auto-power  $P_{22}$  with  $t = 0, 1$ . The highest detection significance is in the  $t = 1$  configuration, where the combined detection significance is  $> 15\sigma$ .

Our results show that future galaxy surveys, and even more their multi-tracer combination, should be able to detect the combined relativistic and wide-angle contributions to the power spectra, assuming that other surveys can measure the clustering, evolution and magnification biases with reasonable uncertainties – and also assuming that ultra-large scale systematics can be dealt with. This detectability is dependent on the choice of the line-of-sight parameter  $t$ , with the strongest detectability for  $t = 1$  (see Figure 9). The choice of  $t$  has significant implications for computation, so it is useful that the signal is detectable in all cases we considered. Detectability means that constraints on cosmological parameters could be affected by omitting these corrections to the standard power spectra. In particular, we expect that measurements of the local primordial non-Gaussianity parameter  $f_{\text{NL}}$  could be affected by these corrections. Future work will look at Fisher forecasts on  $f_{\text{NL}}$  and other cosmological parameters [35].

### Acknowledgements

SJ is supported by the Stellenbosch University Astrophysics Research Group fund. SG and RM are supported by the South African Radio Astronomy Observatory and National Research Foundation (grant no. 75415). SC acknowledges support from the Italian Ministry of University and Research, PRIN 2022 ‘EXSKALIBUR – Euclid-Cross-SKA: Likelihood Inference Building for Universe Research’, from the Italian Ministry of Foreign Affairs and International Cooperation (grant no. ZA23GR03), and from the European Union – Next Generation EU.

## A Fourier kernels

$$\begin{aligned} \mathcal{K}_a^{\text{W}} = & \frac{f}{k^2} \left\{ (t - \sigma_a)^2 \left[ (k_x^2 - k_z^2) \epsilon_x^2 + (k_y^2 - k_z^2) \epsilon_y^2 \right. \right. \\ & \left. \left. + 2(k_x k_y \epsilon_x \epsilon_y - k_x k_z \epsilon_x \epsilon_z - k_y k_z \epsilon_y \epsilon_z) \right] \right. \\ & \left. + 2(t - \sigma_a) \left[ k_x k_z \epsilon_x + k_y k_z \epsilon_y \right] \right\} + \mathcal{O}(\epsilon^3), \end{aligned} \quad (\text{A.1})$$

$$\begin{aligned} \mathcal{K}_a^{\text{RW}} = & i \frac{1}{k} \frac{\mathcal{H}}{k} f \left\{ \frac{2(1 - \mathcal{Q}_a)}{r\mathcal{H}} \left[ (t - \sigma_a) k_z \epsilon_z \right. \right. \\ & \left. \left. + \frac{1}{2} (t - \sigma_a)^2 \left( k_z (\epsilon_x^2 + \epsilon_y^2 - 2\epsilon_z^2) + 2(k_x \epsilon_x + k_y \epsilon_y) \epsilon_z \right) \right] \right. \\ & \left. + \left[ 2\mathcal{Q}_a - \mathcal{E}_a + \frac{2(1 - \mathcal{Q}_a)}{r\mathcal{H}} + \frac{\mathcal{H}'}{\mathcal{H}^2} \right] \left[ - (t - \sigma_a) (k_x \epsilon_x + k_y \epsilon_y) \right. \right. \\ & \left. \left. + \frac{1}{2} (t - \sigma_a)^2 \left( k_z (\epsilon_x^2 + \epsilon_y^2) + 2(k_x \epsilon_x + k_y \epsilon_y) \epsilon_z \right) \right] \right\} \\ & + \frac{3}{2} \Omega_m \frac{\mathcal{H}^2}{k^2} \frac{(1 - \mathcal{Q}_a)}{r\mathcal{H}} \left[ 2(t - \sigma_a) \epsilon_z + (t - \sigma_a)^2 (\epsilon_x^2 + \epsilon_y^2 - 2\epsilon_z^2) \right] + \mathcal{O}(\epsilon^3), \end{aligned} \quad (\text{A.2})$$

where  $\sigma_a = (0, 1)$ .

Derivative terms that appear in power spectrum expressions are

$$\partial_k \mathcal{K}_a^{\text{S}} = -b_{a\phi} \frac{f_{\text{NL}}}{\mathcal{M}} \frac{\partial_k \mathcal{M}}{\mathcal{M}} - \frac{2}{k} f \left( \frac{k_z}{k} \right)^2, \quad (\text{A.3})$$

$$\partial_k^2 \mathcal{K}_a^{\text{S}} = 2b_{a\phi} \frac{f_{\text{NL}}}{\mathcal{M}} \frac{(\partial_k \mathcal{M})^2}{\mathcal{M}^2} - b_{a\phi} \frac{f_{\text{NL}}}{\mathcal{M}} \frac{\partial_k^2 \mathcal{M}}{\mathcal{M}} + \frac{6}{k^2} f \left( \frac{k_z}{k} \right)^2, \quad (\text{A.4})$$

$$\partial_{k_z} \mathcal{K}_I^{\text{S}} = \frac{2}{k} f \frac{k_z}{k}, \quad (\text{A.5})$$

$$\partial_{k_z} \partial_k \mathcal{K}_a^{\text{S}} = -\frac{4}{k^2} f \frac{k_z}{k}, \quad (\text{A.6})$$

$$\partial_k \mathcal{K}_a^{\text{D}} = -\frac{2}{k} \mathcal{K}_a^{\text{D}}, \quad (\text{A.7})$$

where  $f_{\text{NL}}$  is the local primordial non-Gaussianity parameter,  $b_{a\phi}$  is the primordial non-Gaussian bias and

$$\mathcal{M}(k, z) = \frac{2D(z) T(k) k^2}{3\Omega_{m0} H_0^2 g_{\text{dec}}}. \quad (\text{A.8})$$

Here  $D$  is the linear growth factor, normalised to 1 at  $z = 0$ ,  $T(k)$  is the matter transfer function, normalised to 1 at  $k = 0$ , and  $g_{\text{dec}}$  is the metric potential growth factor at decoupling.

## B Coefficients $C_{lmn}^{(ab)}$

$$C_{000}^{(ab)} = \mathcal{K}_a^S \mathcal{K}_b^S + \mathcal{K}_a^D \mathcal{K}_b^{D*} + \mathcal{K}_a^S \mathcal{K}_b^{D*} + \mathcal{K}_b^S \mathcal{K}_a^D + \mathcal{K}_a^S \mathcal{K}_b^\Phi + \mathcal{K}_b^S \mathcal{K}_a^\Phi \quad (\text{B.1})$$

$$C_{001}^{(ab)} = \frac{1}{(kr)} \left\{ 3\Omega_m \left( \frac{\mathcal{H}}{k} \right) \left[ t(1 - \mathcal{Q}_b) \mathcal{K}_a^S - (1 - t)(1 - \mathcal{Q}_a) \mathcal{K}_b^S \right] \right. \\ \left. - i 2f \frac{k_z}{k} \left[ (1 - t)(1 - \mathcal{Q}_a) (\mathcal{K}_b^S + \mathcal{K}_b^{D*}) + t(1 - \mathcal{Q}_b) (\mathcal{K}_a^S + \mathcal{K}_a^D) \right] \right\} \quad (\text{B.2})$$

$$C_{010}^{(ab)} = 2f \frac{k_y}{k} \frac{k_z}{k} \left[ t (\mathcal{K}_a^S + \mathcal{K}_a^D + \mathcal{K}_a^\Phi) - (1 - t) (\mathcal{K}_b^S + \mathcal{K}_b^{D*} + \mathcal{K}_b^\Phi) \right] \quad (\text{B.3})$$

$$+ i f \frac{k_y}{k} \left\{ \frac{2}{(kr)} \left[ t(1 - \mathcal{Q}_b) (\mathcal{K}_a^S + \mathcal{K}_a^D) + (1 - t)(1 - \mathcal{Q}_a) (\mathcal{K}_b^S + \mathcal{K}_b^{D*}) \right] \right. \\ \left. + \left( \frac{\mathcal{H}}{k} \right) \left[ (1 - t) \left( -\varepsilon_a + 2\mathcal{Q}_a + \frac{\mathcal{H}'}{\mathcal{H}^2} \right) (\mathcal{K}_b^S + \mathcal{K}_b^{D*}) \right. \right. \\ \left. \left. + t \left( -\varepsilon_b + 2\mathcal{Q}_b + \frac{\mathcal{H}'}{\mathcal{H}^2} \right) (\mathcal{K}_a^S + \mathcal{K}_a^D) \right] \right\} \quad (\text{B.4})$$

$$C_{100}^{(ab)} = C_{010}^{(ab)} \Big|_{k_y \rightarrow k_x} \quad (\text{B.5})$$

$$C_{011}^{(ab)} = -2f \frac{k_y}{k} \frac{k_z}{k} \left\{ (1 - t)^2 (\mathcal{K}_b^S + \mathcal{K}_b^{D*} + \mathcal{K}_b^\Phi) + t^2 (\mathcal{K}_a^S + \mathcal{K}_a^D + \mathcal{K}_a^\Phi) \right. \\ \left. - \frac{1}{(kr)} \left( \frac{\mathcal{H}}{k} \right) t(1 - t) \left[ -3\Omega_m (2 - \mathcal{Q}_a - \mathcal{Q}_b) \right. \right. \\ \left. \left. + f \left[ \left( -\varepsilon_b + 2\mathcal{Q}_b + \frac{\mathcal{H}'}{\mathcal{H}^2} \right) (1 - \mathcal{Q}_a) \right. \right. \right. \\ \left. \left. \left. + \left( -\varepsilon_a + 2\mathcal{Q}_a + \frac{\mathcal{H}'}{\mathcal{H}^2} \right) (1 - \mathcal{Q}_b) \right] \right] \right. \\ \left. - \frac{1}{(kr)^2} 4f t(1 - t)(1 - \mathcal{Q}_a)(1 - \mathcal{Q}_b) \right\} \\ + i f \frac{k_y}{k} \left\{ \frac{4}{(kr)} \left[ f \left( \frac{k_z}{k} \right)^2 t(1 - t)(\mathcal{Q}_a - \mathcal{Q}_b) + (1 - t)^2 (1 - \mathcal{Q}_a) (\mathcal{K}_b^S + \mathcal{K}_b^{D*}) \right. \right. \\ \left. \left. - t^2 (1 - \mathcal{Q}_b) (\mathcal{K}_a^S + \mathcal{K}_a^D) \right] \right. \\ \left. + \left( \frac{\mathcal{H}}{k} \right) \left[ (1 - t)^2 \left( -\varepsilon_a + 2\mathcal{Q}_a + \frac{\mathcal{H}'}{\mathcal{H}^2} \right) (\mathcal{K}_b^S + \mathcal{K}_b^{D*}) \right. \right. \\ \left. \left. - t^2 \left( -\varepsilon_b + 2\mathcal{Q}_b + \frac{\mathcal{H}'}{\mathcal{H}^2} \right) (\mathcal{K}_a^S + \mathcal{K}_a^D) \right] \right\} \quad (\text{B.6})$$

$$C_{101}^{(ab)} = C_{011}^{(ab)} \Big|_{k_y \rightarrow k_x} \quad (\text{B.7})$$

$$\begin{aligned}
C_{110}^{(ab)} = & 2f \frac{k_x}{k} \frac{k_y}{k} \left\{ (1-t)^2 (\mathcal{K}_b^S + \mathcal{K}_b^{D*} + \mathcal{K}_b^\Phi) + t^2 (\mathcal{K}_a^S + \mathcal{K}_a^D + \mathcal{K}_a^\Phi) \right. \\
& - f t(1-t) \left[ 4 \left( \frac{k_z}{k} \right)^2 + \left( \frac{\mathcal{H}}{k} \right)^2 \left[ (2\mathcal{Q}_b - \mathcal{E}_b)(2\mathcal{Q}_a - \mathcal{E}_a) \right. \right. \\
& \qquad \qquad \qquad \left. \left. + \frac{\mathcal{H}'}{\mathcal{H}^2} \left( -\mathcal{E}_a - \mathcal{E}_b + 2(\mathcal{Q}_a + \mathcal{Q}_b) + \frac{\mathcal{H}'}{\mathcal{H}^2} \right) \right] \right. \\
& \qquad \qquad \qquad \left. + \frac{2}{(kr)} \left( \frac{\mathcal{H}}{k} \right) \left[ \left( -\mathcal{E}_b + 2\mathcal{Q}_b + \frac{\mathcal{H}'}{\mathcal{H}^2} \right) (1 - \mathcal{Q}_a) \right. \right. \\
& \qquad \qquad \qquad \left. \left. + \left( -\mathcal{E}_a + 2\mathcal{Q}_a + \frac{\mathcal{H}'}{\mathcal{H}^2} \right) (1 - \mathcal{Q}_b) \right] \right. \\
& \qquad \qquad \qquad \left. + \frac{4}{(kr)^2} (1 - \mathcal{Q}_b)(1 - \mathcal{Q}_a) \right] \\
& \left. + i 2f \frac{k_z}{k} t(1-t) \left[ \left( \frac{\mathcal{H}}{k} \right) [\mathcal{E}_b - \mathcal{E}_a - 2(\mathcal{Q}_b - \mathcal{Q}_a)] + \frac{2}{(kr)} (\mathcal{Q}_b - \mathcal{Q}_a) \right] \right\} \quad (\text{B.8})
\end{aligned}$$

$$\begin{aligned}
C_{002}^{(ab)} = & -\frac{3}{(kr)} \left( \frac{\mathcal{H}}{k} \right) \Omega_m \left[ (1-t)^2 (1 - \mathcal{Q}_a) \mathcal{K}_b^S + t^2 (1 - \mathcal{Q}_b) \mathcal{K}_a^S \right] \\
& - \frac{4}{(kr)^2} f^2 \left( \frac{k_z}{k} \right)^2 t(1-t)(1 - \mathcal{Q}_a)(1 - \mathcal{Q}_b) \\
& + i \frac{2}{(kr)} f \frac{k_z}{k} \left[ t^2 (1 - \mathcal{Q}_b) (\mathcal{K}_a^S + \mathcal{K}_a^D) - (1-t)^2 (1 - \mathcal{Q}_a) (\mathcal{K}_b^S + \mathcal{K}_b^{D*}) \right] \quad (\text{B.9})
\end{aligned}$$

$$\begin{aligned}
C_{020}^{(ab)} = & f \left[ \left( \frac{k_y}{k} \right)^2 - \left( \frac{k_z}{k} \right)^2 \right] \left[ t^2 (\mathcal{K}_a^S + \mathcal{K}_a^D + \mathcal{K}_a^\Phi) + (1-t)^2 (\mathcal{K}_b^S + \mathcal{K}_b^{D*} + \mathcal{K}_b^\Phi) \right] \\
& + \frac{1}{(kr)} \left( \frac{\mathcal{H}}{k} \right) \frac{3}{2} \Omega_m \left[ t^2 (1 - \mathcal{Q}_b) \mathcal{K}_a^S + (1-t)^2 (1 - \mathcal{Q}_a) \mathcal{K}_b^S \right] \\
& - f^2 t(1-t) \left( \frac{k_y}{k} \right)^2 \left\{ 4 \left( \frac{k_z}{k} \right)^2 + \left( \frac{\mathcal{H}}{k} \right)^2 \left[ (2\mathcal{Q}_b - \mathcal{E}_b)(2\mathcal{Q}_a - \mathcal{E}_a) \right. \right. \\
& \qquad \qquad \qquad \left. \left. + \frac{\mathcal{H}'}{\mathcal{H}^2} \left( -\mathcal{E}_a - \mathcal{E}_b + 2(\mathcal{Q}_a + \mathcal{Q}_b) + \frac{\mathcal{H}'}{\mathcal{H}^2} \right) \right] \right. \\
& \qquad \qquad \qquad \left. + \frac{2}{(kr)} \left( \frac{\mathcal{H}}{k} \right) \left[ \left( -\mathcal{E}_b + 2\mathcal{Q}_b + \frac{\mathcal{H}'}{\mathcal{H}^2} \right) (1 - \mathcal{Q}_a) \right. \right. \\
& \qquad \qquad \qquad \left. \left. + \left( -\mathcal{E}_a + 2\mathcal{Q}_a + \frac{\mathcal{H}'}{\mathcal{H}^2} \right) (1 - \mathcal{Q}_b) \right] \right. \\
& \qquad \qquad \qquad \left. + \frac{4}{(kr)^2} (1 - \mathcal{Q}_b)(1 - \mathcal{Q}_a) \right\} \\
& + i f \left( \frac{k_z}{k} \right) \left\{ 2f \left( \frac{k_y}{k} \right)^2 t(1-t) \left[ \left( \frac{\mathcal{H}}{k} \right) [\mathcal{E}_b - \mathcal{E}_a - 2(\mathcal{Q}_b - \mathcal{Q}_a)] + \frac{2}{(kr)} (\mathcal{Q}_b - \mathcal{Q}_a) \right] \right. \\
& \qquad \qquad \qquad + \frac{1}{2} \left( \frac{\mathcal{H}}{k} \right) \left[ (1-t)^2 \left( -\mathcal{E}_a + 2\mathcal{Q}_a + \frac{\mathcal{H}'}{\mathcal{H}^2} \right) (\mathcal{K}_b^S + \mathcal{K}_b^{D*}) \right. \\
& \qquad \qquad \qquad \left. \left. - t^2 \left( -\mathcal{E}_b + 2\mathcal{Q}_b + \frac{\mathcal{H}'}{\mathcal{H}^2} \right) (\mathcal{K}_a^S + \mathcal{K}_a^D) \right] \right. \\
& \qquad \qquad \qquad \left. + \frac{2}{(kr)} \left[ (1-t)^2 (1 - \mathcal{Q}_a) (\mathcal{K}_b^S + \mathcal{K}_b^{D*}) - t^2 (1 - \mathcal{Q}_b) (\mathcal{K}_a^S + \mathcal{K}_a^D) \right] \right\} \quad (\text{B.10})
\end{aligned}$$

$$C_{200}^{(ab)} = C_{020}^{(ab)} \Big|_{k_y \rightarrow k_x} \quad (\text{B.11})$$

## C Multipoles of the power spectra

The monopoles ( $\ell = 0$ ) for the standard, relativistic, wide-angle and cross-terms from wide-angle and relativistic contributions are

$$P_{ab}^{\text{S}(0)} = \left[ \hat{b}_a \hat{b}_b + \frac{f}{3} (\hat{b}_a + \hat{b}_b) + \frac{f^2}{5} \right] P, \quad (\text{C.1})$$

$$P_{ab}^{\text{R}(0)} = \left[ \frac{1}{3} \frac{1}{k^2} \gamma_a^{\text{D}} \gamma_b^{\text{D}} + \left( \frac{f}{3} + \hat{b}_b \right) \frac{1}{k^2} \gamma_a^{\Phi} + \left( \frac{f}{3} + \hat{b}_a \right) \frac{1}{k^2} \gamma_b^{\Phi} \right] P, \quad (\text{C.2})$$

$$\begin{aligned} P_{ab}^{\text{W}(0)} = & \frac{2}{105} \frac{f}{(kr)^2} \left\{ f[1 + 18t(1-t)] - 21[(1-t)^2 \hat{b}_b + t^2 \hat{b}_a] \right. \\ & - 35[(1-t)^2 k \partial_k \hat{b}_b + t^2 k \partial_k \hat{b}_a] \\ & \left. - 7[(1-t)^2 k^2 \partial_k^2 \hat{b}_b + t^2 k^2 \partial_k^2 \hat{b}_a] \right\} P \\ & + \left\{ f[11 + 30t(1-t)] - 35[(1-t)^2 \hat{b}_b + t^2 \hat{b}_a] \right. \\ & \left. - 14[(1-t)^2 k \partial_k \hat{b}_b + t^2 k \partial_k \hat{b}_a] \right\} k \partial_k P \\ & + \left\{ f[5 + 6t(1-t)] - 7[(1-t)^2 \hat{b}_b + t^2 \hat{b}_a] \right\} k^2 \partial_k^2 P \Big\}, \quad (\text{C.3}) \end{aligned}$$

$$\begin{aligned} P_{ab}^{\text{RW}(0)}(k) = & \frac{2}{15} f \left\{ - \frac{2}{kr} \left[ (1-t) \frac{1}{k} \gamma_b^{\text{D}} + t \frac{1}{k} \gamma_a^{\text{D}} \right] \right. \\ & + \frac{1}{kr} \frac{\mathcal{H}}{k} \left[ (1-t)(f + 5\hat{b}_b) \left( \mathcal{E}_a - 2\mathcal{Q}_a - \frac{\mathcal{H}'}{\mathcal{H}^2} \right) \right. \\ & \left. \left. + t(f + 5\hat{b}_a) \left( \mathcal{E}_b - 2\mathcal{Q}_b - \frac{\mathcal{H}'}{\mathcal{H}^2} \right) \right] \right. \\ & + \frac{5}{kr} \frac{\mathcal{H}}{k} \left[ (1-t) \left( \mathcal{E}_a - 2\mathcal{Q}_a - \frac{\mathcal{H}'}{\mathcal{H}^2} \right) k \partial_k \hat{b}_b \right. \\ & \left. \left. + t \left( \mathcal{E}_b - 2\mathcal{Q}_b - \frac{\mathcal{H}'}{\mathcal{H}^2} \right) k \partial_k \hat{b}_a \right] \right. \\ & + \frac{1}{(kr)^2} \left[ (1-t)(1 - \mathcal{Q}_a)(f - 5\hat{b}_b) + t(1 - \mathcal{Q}_b)(f - 5\hat{b}_a) \right] \\ & \left. - \frac{5}{(kr)^2} \left[ (1-t)(1 - \mathcal{Q}_a) k \partial_k \hat{b}_b + t(1 - \mathcal{Q}_b) k \partial_k \hat{b}_a \right] \right\} P \\ & + \frac{2}{15} f \left\{ - \frac{2}{kr} \left[ (1-t) \frac{1}{k} \gamma_b^{\text{D}} + t \frac{1}{k} \gamma_a^{\text{D}} \right] \right. \\ & \left. + \frac{1}{kr} \frac{\mathcal{H}}{k} \left[ (1-t)(f + 5\hat{b}_b) \left( \mathcal{E}_a - 2\mathcal{Q}_a - \frac{\mathcal{H}'}{\mathcal{H}^2} \right) \right] \right\} \end{aligned}$$

$$\begin{aligned}
& + t(f + 5\hat{b}_a) \left( \mathcal{E}_b - 2\mathcal{Q}_b - \frac{\mathcal{H}'}{\mathcal{H}^2} \right) \Big] \\
& + \frac{1}{(kr)^2} \left[ (1-t)(1-\mathcal{Q}_a)(f - 5\hat{b}_b) + t(1-\mathcal{Q}_b)(f - 5\hat{b}_a) \right] \Big\} k \partial_k P \\
& + \frac{1}{15} \frac{f}{(kr)^2} \left\{ -2 \left[ (1-t)^2 \frac{1}{k^2} \gamma_b^\Phi + t^2 \frac{1}{k^2} \gamma_a^\Phi \right] \right. \\
& \quad + 3 \frac{\mathcal{H}}{k} \left[ (1-t)^2 \left( \mathcal{E}_a - 2\mathcal{Q}_a - \frac{\mathcal{H}'}{\mathcal{H}^2} \right) \frac{1}{k} \gamma_b^D \right. \\
& \quad \quad \left. \left. + t^2 \left( \mathcal{E}_b - 2\mathcal{Q}_b - \frac{\mathcal{H}'}{\mathcal{H}^2} \right) \frac{1}{k} \gamma_a^D \right] \right. \\
& \quad \left. + 8(1-t)t \frac{\mathcal{H}^2}{k^2} f \left( \mathcal{E}_b - 2\mathcal{Q}_b - \frac{\mathcal{H}'}{\mathcal{H}^2} \right) \left( \mathcal{E}_a - 2\mathcal{Q}_a - \frac{\mathcal{H}'}{\mathcal{H}^2} \right) \right\} k^2 \partial_k^2 P, \tag{C.4}
\end{aligned}$$

where

$$\hat{b}_a = b_a + f_{\text{NL}} \frac{b_{a\phi}}{\mathcal{M}}. \tag{C.5}$$

The dipoles ( $\ell = 1$ ) for each contribution are

$$P_{ab}^{\text{S}(1)} = 0, \tag{C.6}$$

$$P_{ab}^{\text{R}(1)} = i \frac{1}{5} \left[ (3f + 5\hat{b}_b) \frac{1}{k} \gamma_a^D - (3f + 5\hat{b}_a) \frac{1}{k} \gamma_b^D \right] P, \tag{C.7}$$

$$\begin{aligned}
P_{ab}^{\text{W}(1)} = & -i \frac{4}{35} \frac{f}{kr} \left\{ \left[ 9(1-2t)f + 21 \left[ (1-t)\hat{b}_b - t\hat{b}_a \right] \right. \right. \\
& \quad \left. \left. + 7 \left[ (1-t)k \partial_k \hat{b}_b - tk \partial_k \hat{b}_a \right] \right] P \right. \\
& \quad \left. + \left[ 3(1-2t)f + 7 \left[ (1-t)\hat{b}_b - t\hat{b}_a \right] \right] k \partial_k P \right\}, \tag{C.8}
\end{aligned}$$

$$\begin{aligned}
P_{ab}^{\text{RW}(1)} = & i \frac{1}{5} \frac{1}{(kr)^2} \frac{\mathcal{H}}{k} \left\{ -15\Omega_m \left[ (1-t)(1-\mathcal{Q}_a)k \partial_k \hat{b}_b - t(1-\mathcal{Q}_b)k \partial_k \hat{b}_a \right] \right. \\
& \quad + 3f \left[ (1-t)^2 \left( \mathcal{E}_a - 2\mathcal{Q}_a - \frac{\mathcal{H}'}{\mathcal{H}^2} \right) k^2 \partial_k^2 \hat{b}_b \right. \\
& \quad \quad \left. \left. - t^2 \left( \mathcal{E}_b - 2\mathcal{Q}_b - \frac{\mathcal{H}'}{\mathcal{H}^2} \right) k^2 \partial_k^2 \hat{b}_a \right] \right\} P \\
& + i \frac{1}{5} \left\{ -4 \frac{f}{kr} \left[ (1-t) \frac{1}{k^2} \gamma_b^\Phi - t \frac{1}{k^2} \gamma_a^\Phi \right] \right. \\
& \quad \left. - 2 \frac{f}{kr} \frac{\mathcal{H}}{k} \left[ (1-t) \left( \mathcal{E}_a - 2\mathcal{Q}_a - \frac{\mathcal{H}'}{\mathcal{H}^2} \right) \frac{1}{k} \gamma_b^D - t \left( \mathcal{E}_b - 2\mathcal{Q}_b - \frac{\mathcal{H}'}{\mathcal{H}^2} \right) \frac{1}{k} \gamma_a^D \right] \right\}
\end{aligned}$$

$$\begin{aligned}
& + \frac{2}{7} \frac{f}{(kr)^2} \frac{\mathcal{H}}{k} \left[ (1-t)(21t+5)f \left( \mathcal{E}_a - 2\mathcal{Q}_a - \frac{\mathcal{H}'}{\mathcal{H}^2} \right) \right. \\
& \quad \left. + t(21t-26)f \left( \mathcal{E}_b - 2\mathcal{Q}_b - \frac{\mathcal{H}'}{\mathcal{H}^2} \right) \right. \\
& + 21(1-t)^2 \left( \mathcal{E}_a - 2\mathcal{Q}_a - \frac{\mathcal{H}'}{\mathcal{H}^2} \right) k \partial_k \hat{b}_b - 21t^2 \left( \mathcal{E}_b - 2\mathcal{Q}_b - \frac{\mathcal{H}'}{\mathcal{H}^2} \right) k \partial_k \hat{b}_a \left. \right] \\
& - \frac{6}{7} \frac{f}{(kr)^2} \left[ - (1-t)^2 \frac{1}{k} \gamma_b^D + t^2 \frac{1}{k} \gamma_a^D \right] \\
& - \frac{3}{(kr)^2} \frac{\mathcal{H}}{k} \Omega_m \left[ (1-t)(1-\mathcal{Q}_a)(3f+5\hat{b}_b) - t(1-\mathcal{Q}_b)(3f+5\hat{b}_a) \right] \\
& - 2 \frac{f}{(kr)^2} \left[ (1-t)(1-\mathcal{Q}_a) \frac{1}{k} \gamma_b^D - t(1-\mathcal{Q}_b) \frac{1}{k} \gamma_a^D \right] \left. \right\} k \partial_k P \\
& + i \frac{1}{35} \frac{f}{(kr)^2} \left\{ \frac{\mathcal{H}}{k} \left[ (1-t)(7t+9)f \left( \mathcal{E}_a - 2\mathcal{Q}_a - \frac{\mathcal{H}'}{\mathcal{H}^2} \right) + t(7t-16)f \left( \mathcal{E}_b - 2\mathcal{Q}_b - \frac{\mathcal{H}'}{\mathcal{H}^2} \right) \right. \right. \\
& \quad \left. + 21(1-t)^2 \left( \mathcal{E}_a - 2\mathcal{Q}_a - \frac{\mathcal{H}'}{\mathcal{H}^2} \right) \hat{b}_b - 21t^2 \left( \mathcal{E}_b - 2\mathcal{Q}_b - \frac{\mathcal{H}'}{\mathcal{H}^2} \right) \hat{b}_a \right] \\
& \quad \left. - 10 \left[ (1-t)^2 \frac{1}{k} \gamma_b^D - t^2 \frac{1}{k} \gamma_a^D \right] \right\} k^2 \partial_k^2 P . \tag{C.9}
\end{aligned}$$

The quadrupoles ( $\ell = 2$ ) are

$$P_{ab}^{S(2)} = \frac{2}{21} f \left[ 6f + 7\hat{b}_a + 7\hat{b}_b \right] P , \tag{C.10}$$

$$P_{ab}^{R(2)} = \frac{2}{3} \left[ \frac{1}{k^2} \gamma_a^D \gamma_b^D + f \frac{1}{k^2} \gamma_a^\Phi + f \frac{1}{k^2} \gamma_b^\Phi \right] P , \tag{C.11}$$

$$\begin{aligned}
P_{ab}^{W(2)} = \frac{2}{21} \frac{f}{(kr)^2} \left\{ \right. & \left. \left\{ 2f[-13 + 54t(1-t)] - 66 \left[ (1-t)^2 \hat{b}_b + t^2 \hat{b}_a \right] \right. \right. \\
& + 22 \left[ (1-t)^2 k \partial_k \hat{b}_b + t^2 k \partial_k \hat{b}_a \right] \\
& \left. + 11 \left[ (1-t)^2 k^2 \partial_k^2 \hat{b}_b + t^2 k^2 \partial_k^2 \hat{b}_a \right] \right\} P \\
& + 2 \left\{ 11 \left[ (1-t)^2 k \partial_k \hat{b}_b + t^2 k \partial_k \hat{b}_a \right] + 2f[2 + 3t(1-t)] \right. \\
& \left. + 11 \left[ (1-t)^2 \hat{b}_b + t^2 \hat{b}_a \right] \right\} k \partial_k P \tag{C.12}
\end{aligned}$$

$$+ \left\{ 3f[1 - 2t(1-t)] + 11 \left[ (1-t)^2 \hat{b}_b + t^2 \hat{b}_a \right] \right\} k^2 \partial_k^2 P \left. \right\} , \tag{C.13}$$

$$\begin{aligned}
P_{ab}^{RW(2)}(k) = \frac{2}{21} f \left\{ \right. & \left. \frac{2}{kr} \frac{\mathcal{H}}{k} \left[ (1-t)(5f + 7\hat{b}_b) \left( \mathcal{E}_a - 2\mathcal{Q}_a - \frac{\mathcal{H}'}{\mathcal{H}^2} \right) \right. \right. \\
& \left. + t(5f + 7\hat{b}_a) \left( \mathcal{E}_b - 2\mathcal{Q}_b - \frac{\mathcal{H}'}{\mathcal{H}^2} \right) \right] \\
& \left. - \frac{7}{kr} \frac{\mathcal{H}}{k} \left[ (1-t) \left( \mathcal{E}_a - 2\mathcal{Q}_a - \frac{\mathcal{H}'}{\mathcal{H}^2} \right) k \partial_k \hat{b}_b \right. \right.
\end{aligned}$$

$$\begin{aligned}
& + t \left( \mathcal{E}_b - 2\mathcal{Q}_b - \frac{\mathcal{H}'}{\mathcal{H}^2} \right) k \partial_k \hat{b}_a \Big] \\
& - \frac{20}{kr} \left[ (1-t) \frac{1}{k} \gamma_b^D + t \frac{1}{k} \gamma_a^D \right] \\
& + \frac{28}{(kr)^2} \left[ (1-t)(1-\mathcal{Q}_a) k \partial_k \hat{b}_b + t(1-\mathcal{Q}_b) k \partial_k \hat{b}_a \right] \\
& - \frac{2}{(kr)^2} \left[ (1-t)(1-\mathcal{Q}_a)(13f + 28\hat{b}_b) \right. \\
& \quad \left. + t(1-\mathcal{Q}_b)(13f + 28\hat{b}_a) \right] \Big\} P \\
& + \frac{2}{21} f \left\{ \frac{1}{kr} \frac{\mathcal{H}}{k} \left[ (1-t)(f - 7\hat{b}_b) \left( \mathcal{E}_a - 2\mathcal{Q}_a - \frac{\mathcal{H}'}{\mathcal{H}^2} \right) \right. \right. \\
& \quad \left. \left. + t(f - 7\hat{b}_a) \left( \mathcal{E}_b - 2\mathcal{Q}_b - \frac{\mathcal{H}'}{\mathcal{H}^2} \right) \right] \right. \\
& \quad - \frac{2}{kr} \left[ (1-t) \frac{1}{k} \gamma_b^D + t \frac{1}{k} \gamma_a^D \right] \\
& \quad \left. + \frac{2}{(kr)^2} \left[ (1-t)(1-\mathcal{Q}_a)(5f + 14\hat{b}_b) \right. \right. \\
& \quad \left. \left. + t(1-\mathcal{Q}_b)(5f + 14\hat{b}_a) \right] \right\} k \partial_k P \\
& + \frac{1}{21} \frac{f}{(kr)^2} \left\{ -16(1-t)t \frac{\mathcal{H}^2}{k^2} f \left( \mathcal{E}_a - 2\mathcal{Q}_a - \frac{\mathcal{H}'}{\mathcal{H}^2} \right) \left( \mathcal{E}_b - 2\mathcal{Q}_b - \frac{\mathcal{H}'}{\mathcal{H}^2} \right) \right. \\
& \quad + 3 \frac{\mathcal{H}}{k} \left[ (1-t)^2 \left( \mathcal{E}_a - 2\mathcal{Q}_a - \frac{\mathcal{H}'}{\mathcal{H}^2} \right) \frac{1}{k} \gamma_b^D \right. \\
& \quad \left. \left. + t^2 \left( \mathcal{E}_b - 2\mathcal{Q}_b - \frac{\mathcal{H}'}{\mathcal{H}^2} \right) \frac{1}{k} \gamma_a^D \right] \right. \\
& \quad \left. + 22 \left[ (1-t)^2 \frac{1}{k^2} \gamma_b^\Phi + t^2 \frac{1}{k^2} \gamma_a^\Phi \right] \right\} k^2 \partial_k^2 P . \tag{C.14}
\end{aligned}$$



## References

- [1] P. McDonald, *Gravitational redshift and other redshift-space distortions of the imaginary part of the power spectrum*, *JCAP* **0911** (2009) 026, [[arXiv:0907.5220](#)].
- [2] J. Yoo, *General Relativistic Description of the Observed Galaxy Power Spectrum: Do We Understand What We Measure?*, *Phys. Rev.* **D82** (2010) 083508, [[arXiv:1009.3021](#)].
- [3] C. Bonvin and R. Durrer, *What galaxy surveys really measure*, *Phys. Rev.* **D84** (2011) 063505, [[arXiv:1105.5280](#)].
- [4] A. Challinor and A. Lewis, *The linear power spectrum of observed source number counts*, *Phys. Rev.* **D84** (2011) 043516, [[arXiv:1105.5292](#)].
- [5] D. Bertacca, R. Maartens, A. Raccanelli, and C. Clarkson, *Beyond the plane-parallel and Newtonian approach: Wide-angle redshift distortions and convergence in general relativity*, *JCAP* **1210** (2012) 025, [[arXiv:1205.5221](#)].
- [6] J. Yoo and U. Seljak, *Wide Angle Effects in Future Galaxy Surveys*, *Mon. Not. Roy. Astron. Soc.* **447** (2015), no. 2 1789–1805, [[arXiv:1308.1093](#)].
- [7] V. Tansella, G. Jelic-Cizmek, C. Bonvin, and R. Durrer, *COFFE: a code for the full-sky relativistic galaxy correlation function*, *JCAP* **10** (2018) 032, [[arXiv:1806.11090](#)].
- [8] H. S. G. Gebhardt and O. Doré, *Fabulous code for spherical Fourier-Bessel decomposition*, *Phys. Rev. D* **104** (2021), no. 12 123548, [[arXiv:2102.10079](#)].
- [9] A. S. Szalay, T. Matsubara, and S. D. Landy, *Redshift space distortions of the correlation function in wide angle galaxy surveys*, *Astrophys. J. Lett.* **498** (1998) L1, [[astro-ph/9712007](#)].
- [10] S. Bharadwaj, *Radial Redshift Space Distortions*, *Astrophys. J.* **516** (1999) 507–518, [[astro-ph/9812274](#)].
- [11] T. Matsubara, *The Correlation function in redshift space: General formula with wide angle effects and cosmological distortions*, *Astrophys. J.* **535** (2000) 1, [[astro-ph/9908056](#)].
- [12] I. Szapudi, *Wide angle redshift distortions revisited*, *Astrophys. J.* **614** (2004) 51–55, [[astro-ph/0404477](#)].
- [13] P. Papai and I. Szapudi, *Non-Perturbative Effects of Geometry in Wide-Angle Redshift Distortions*, *Mon. Not. Roy. Astron. Soc.* **389** (2008) 292, [[arXiv:0802.2940](#)].
- [14] A. Raccanelli, L. Samushia, and W. J. Percival, *Simulating Redshift-Space Distortions for Galaxy Pairs with Wide Angular Separation*, *Mon. Not. Roy. Astron. Soc.* **409** (2010) 1525, [[arXiv:1006.1652](#)].
- [15] P. H. F. Reimberg, F. Bernardeau, and C. Pitrou, *Redshift-space distortions with wide angular separations*, *JCAP* **1601** (2016), no. 01 048, [[arXiv:1506.06596](#)].
- [16] E. Castorina and M. White, *Beyond the plane-parallel approximation for redshift surveys*, *Mon. Not. Roy. Astron. Soc.* **476** (2018), no. 4 4403–4417, [[arXiv:1709.09730](#)].
- [17] J. N. Benabou, I. Sands, H. S. G. Gebhardt, C. Heinrich, and O. Doré, *Wide-Angle Effects in the Power Spectrum Multipoles in Next-Generation Redshift Surveys*, [[arXiv:2404.04811](#)].
- [18] N. Grimm, F. Scaccabarozzi, J. Yoo, S. G. Biern, and J.-O. Gong, *Galaxy Power Spectrum in General Relativity*, *JCAP* **11** (2020) 064, [[arXiv:2005.06484](#)].
- [19] F. Beutler, E. Castorina, and P. Zhang, *Interpreting measurements of the anisotropic galaxy power spectrum*, *JCAP* **03** (2019) 040, [[arXiv:1810.05051](#)].
- [20] E. Castorina and E. di Dio, *The observed galaxy power spectrum in General Relativity*, *JCAP* **01** (2022), no. 01 061, [[arXiv:2106.08857](#)].

- [21] M. Y. Elkhatab, C. Porciani, and D. Bertacca, *The large-scale monopole of the power spectrum in a Euclid-like survey: wide-angle effects, lensing, and the ‘finger of the observer’*, *Mon. Not. Roy. Astron. Soc.* **509** (2021), no. 2 1626–1645, [[arXiv:2108.13424](#)].
- [22] M. Noorikuhani and R. Scoccimarro, *Wide-angle and relativistic effects in Fourier-space clustering statistics*, *Phys. Rev. D* **107** (2023), no. 8 083528, [[arXiv:2207.12383](#)].
- [23] P. Paul, C. Clarkson, and R. Maartens, *Wide-angle effects in multi-tracer power spectra with Doppler corrections*, *JCAP* **04** (2023) 067, [[arXiv:2208.04819](#)].
- [24] R. Maartens, J. Fonseca, S. Camera, S. Jolicoeur, J.-A. Viljoen, and C. Clarkson, *Magnification and evolution biases in large-scale structure surveys*, *JCAP* **12** (2021), no. 12 009, [[arXiv:2107.13401](#)].
- [25] M. Bruni, R. Crittenden, K. Koyama, R. Maartens, C. Pitrou, and D. Wands, *Disentangling non-Gaussianity, bias and GR effects in the galaxy distribution*, *Phys. Rev. D* **85** (2012) 041301, [[arXiv:1106.3999](#)].
- [26] F. Montano and S. Camera, *Detecting Relativistic Doppler in Galaxy Clustering with Tailored Galaxy Samples*, [arXiv:2309.12400](#).
- [27] C. Bonvin, L. Hui, and E. Gaztanaga, *Asymmetric galaxy correlation functions*, *Phys. Rev. D* **89** (2014), no. 8 083535, [[arXiv:1309.1321](#)].
- [28] C. Bonvin, L. Hui, and E. Gaztanaga, *Optimising the measurement of relativistic distortions in large-scale structure*, *JCAP* **1608** (2016), no. 08 021, [[arXiv:1512.03566](#)].
- [29] E. Gaztanaga, C. Bonvin, and L. Hui, *Measurement of the dipole in the cross-correlation function of galaxies*, *JCAP* **1701** (2017), no. 01 032, [[arXiv:1512.03918](#)].
- [30] V. Irsic, E. Di Dio, and M. Viel, *Relativistic effects in Lyman- $\alpha$  forest*, *JCAP* **1602** (2016), no. 02 051, [[arXiv:1510.03436](#)].
- [31] A. Hall and C. Bonvin, *Measuring cosmic velocities with 21 cm intensity mapping and galaxy redshift survey cross-correlation dipoles*, *Phys. Rev. D* **95** (2017), no. 4 043530, [[arXiv:1609.09252](#)].
- [32] F. Lepori, E. Di Dio, E. Villa, and M. Viel, *Optimal galaxy survey for detecting the dipole in the cross-correlation with 21 cm Intensity Mapping*, *JCAP* **1805** (2018), no. 05 043, [[arXiv:1709.03523](#)].
- [33] C. Bonvin and P. Fleury, *Testing the equivalence principle on cosmological scales*, *JCAP* **1805** (2018), no. 05 061, [[arXiv:1803.02771](#)].
- [34] F. Lepori, V. Iršič, E. Di Dio, and M. Viel, *The impact of relativistic effects on the 3D Quasar-Lyman- $\alpha$  cross-correlation*, *JCAP* **04** (2020) 006, [[arXiv:1910.06305](#)].
- [35] S. Guedezounme, S. Jolicoeur, and R. Maartens, *In preparation*, [arXiv:240n.nnnnn](#).